Published in "Physical Review C 75: 054310, 2007"
which should be cited to refer to this work.

Properties of ^{112}Cd from the $(n, n'\gamma)$ reaction: Lifetimes and transition rates

P. E. Garrett and K. L. Green
Department of Physics, University of Guelph, Guelph, Ontario, N1G2W1 Canada

H. Lehmann*
Institut de Physique, Université de Fribourg, Pérolles, CH-1700 Fribourg, Switzerland

J. Jolie
Institut für Kernphysik, Universtät zu Köln, Zülpicherstrasse 77, D-50937 Köln, Germany

C. A. McGrath,† M. Yeh,‡ and S. W. Yates
Departments of Chemistry and Physics & Astronomy, University of Kentucky, Lexington, Kentucky 40506-0055, USA

Lifetimes of levels below 4 MeV in ^{112}Cd have been measured using the Doppler shift attenuation technique following inelastic scattering of monoenergetic neutrons. Reduced transition rates are determined using the results of previous studies and the current lifetimes. The electromagnetic properties of ^{112}Cd are outlined, and together with results from previous nucleon-transfer studies and inelastic scattering, the levels in ^{112}Cd are interpreted in terms of single-particle configurations and collective excitations, assuming a vibrational model with intruder states. The collective states and their γ-ray decays are compared with IBM-2 model calculations that allow for the mixing between the normal phonon states and intruder configurations. Levels below 1.5 MeV are reproduced reasonably well, whereas at higher excitation energy the calculations fail to reproduce the data in detail.

I. INTRODUCTION

It is of importance to establish benchmark models of nuclear structure against which nuclei can be compared. In most cases, these benchmarks are the results of rather idealized models or calculations since the full nuclear many-body problem is far too complicated to solve. For example, the rotor model [1] serves as the benchmark for collective behavior of well-deformed nuclei and predicts the familiar $I(I+1)$ pattern in the energy sequence for the rotational bands, a pattern followed extremely well. The successes of such simple patterns, as well as the deviations from them, provide insights as to how a strongly-interacting system of fermions organizes. Other benchmarks of collective nuclear structure include the harmonic vibrator [2], and the γ-soft rotor [3]. With the introduction of the interacting boson model (IBM) [4], a new vocabulary was introduced based on the dynamical symmetries of the underlying $U(6)$ group structure; the $SU(3)$ limit, corresponding to rotational nuclei, the $U(5)$ limit, for vibrational nuclei, and the $SO(6)$ limit, corresponding to γ-soft nuclei.

Very early, the Cd isotopes were suggested [5] as paradigms of the $U(5)$ symmetry. The existence of the expected spin multiplets and the nearly harmonic spacing of the energy levels for the two-phonon, and many of the three-phonon, states appeared to leave little doubt. Additional levels in the vicinity of the two-phonon triplet were interpreted [6–8] as intruder configurations involving proton two-particle, two-hole pairs excited across the $Z = 50$ closed shell. Over the years, the modeling [6,9–19] of these states and their interactions have become increasingly sophisticated. With the successful description of the normal phonon and intruder states, the Cd isotopes, especially ^{110,112}Cd, have remained as "among the best $U(5)$ candidates" as cited in the survey by Kern *et al.* [20]. Since this survey was completed, both ^{110}Cd and ^{112}Cd have been studied [21–23] with the $(n, n'\gamma)$ reaction where lifetimes for some members of the proposed three-phonon quintuplet were determined. A series of measurements of lifetimes for the high-spin states in ^{110}Cd have also been reported [24–26]. These studies found that, where measured, proposed three-phonon states indeed had collective decays to assigned two-phonon levels. However, there was evidence, especially in the case of ^{112}Cd, of collective decays [23] to the intruder levels as well, indicating that mixing was taking place. This mixing was taken into account and described within the context of the IBM. Furthermore, a "good" candidate for the 2^+ three-phonon member was lacking, in that decays to the 0^+ two-phonon level were observed but none to the other members of the two-phonon triplet [23]. Even though deviations from the expected $U(5)$ vibrational structure were observed, ^{110,112}Cd have remained as the paradigms of the $U(5)$ symmetry in nuclei.

In the present work, a thorough investigation is performed of the level structure of one of the Cd "paradigms" by considering *all* data available, including new lifetimes measured

*Present address: Swisscom AG, Innovations, CH-3050 Bern, Switzerland.
†Present address: Idaho National Engineering and Environmental Laboratory, P.O. Box 1625, Idaho Falls, Idaho 83415.
‡Present address: Chemistry Department, Brookhaven National Laboratory Upton, NY 11973-5000.

using the $(n, n'\gamma)$ reaction, to examine the extent to which it really satisfies the $U(5)$ limit. Congruent to this is the question of how high in excitation energy the collective states survive, especially as they become embedded in a sea of quasiparticle excitations. ^{112}Cd is an ideal case for such a study since it is one of the paradigms of the $U(5)$ symmetry in nuclei, it has been studied by many complementary means, and it now has one of the best determined level schemes [27]. In the present work, level lifetimes as measured with the Doppler-shift attenuation method (DSAM) following the $(n, n'\gamma)$ reaction are given. Some results from the $(n, n'\gamma)$ reaction study focusing on specific nuclear structure questions have already been published. For example, the investigation of three-phonon states in Ref. [23], the lowest 2^+ mixed-symmetry state in Ref. [28], and the quadrupole-octupole quintuplet in Ref. [29]. The present study thus represents an extension of the previous $(n, n'\gamma)$ results and is an attempt to incorporate data from all previous studies to examine the degree to which ^{112}Cd satisfies the $U(5)$ symmetry limit.

II. EXPERIMENTAL DETAILS

The details of the experiments conducted were given in Ref. [27], and will be only briefly repeated here, concentrating on the aspects related to the extraction of the level lifetimes. The experiments were performed at the 7 MV Van de Graaff accelerator at the University of Kentucky, where the ^{3}H$(p, n)^3$He reaction was used to produce the fast neutrons. Approximately 2 μA of pulsed proton beams (1.875 MHz repetition rate with beam pulses $\sim$ 1 ns in width) impinged on a gas cell containing the ^{3}H gas. The scattering sample consisted of approximately 52.5 g of CdO enriched to 98.18% ^{112}Cd, and was suspended at a distance of 5.5 cm from the end of the gas cell. The full-width-at-half-maximum (FWHM) energy spread of the neutrons striking the sample was $\approx$100 keV for neutron energies used for the present work. The γ-ray spectra were recorded with either 52% or 57% efficient HPGe detectors having resolutions of $\simeq$ 2.1 keV FWHM at 1332 keV. The sample-to-detector distance was typically 1.1 m. Compton suppression was achieved by utilizing an active annular BGO shield, and time-of-flight gating of events related to the beam pulse was used to reduce extraneous background events.

The γ-ray energy calibrations were determined by applying nonlinearity corrections to the peak positions followed by least-squares linear fits to energies of several well-known γ rays, from both ^{112}Cd and sources of ^{60}Co, ^{24}Na, or ^{56}Co, in the in-beam spectra. The nonlinearity curve was determined by using radioactive sources of ^{56}Co and ^{226}Ra placed at the sample position and spectra recorded under identical conditions as the in-beam spectra. The γ-ray angular distributions were measured for incident neutron energies of 2.5 MeV, 3.4 MeV, and 4.2 MeV. Spectra were recorded at 11 angles from (typically) 37° to 155°. The observed γ-ray energies are

$$E_\gamma(\theta) = E_\gamma^o[1 + \beta F(\tau)\cos\theta], \quad (1)$$

where $E_\gamma(\theta)$ is the observed γ-ray energy at an angle θ with respect to the forward recoil direction, taken to be the beam direction, E_γ^o is the unshifted γ-ray energy, and $\beta = v/c$ is the recoil velocity in the center of mass frame. By examining the energy of a γ ray as a function of angle, the attenuation factor $F(\tau)$ can be obtained, and the lifetime τ of the state can be determined [30] by a comparison with the $F(\tau)$ value calculated using the Winterbon formalism [31].

Shown in Fig. 1 are some typical Doppler shift curves determined in the present work. As was shown in Ref. [27], the Doppler shifts are particularly sensitive to the presence of doublets which often cause deviations from linearity when plotted as a function of $\cos\theta$. Some of these effects were displayed in Fig. 8 of Ref. [27].

III. RESULTS

The level lifetimes extracted from the $(n, n'\gamma)$ reaction can be compared with those obtained by other means, such as Coulomb excitation [32–34] (as compiled in the Nuclear Data Sheets [35]) and the (γ, γ') reaction [36,37]. In the former case, the comparison is limited to those levels that were populated with sufficient intensity in the Coulomb excitation process that the matrix elements could be extracted, generally the lowest-lying states, whereas the latter reaction is essentially restricted to spin-1 and 2^+ excitations. Table I lists the lifetimes extracted with the $(n, n'\gamma)$ reaction and those available in the literature obtained by other means. Not included in the $(n, n'\gamma)$ lifetime uncertainty is an estimated 10% uncertainty in the stopping powers. In the (γ, γ') experiments, the measured quantity is the scattering intensity to an excited state s, $I_{s,0}$, given by [36]

$$I_{s,0} = g\left(\pi\frac{\hbar c}{E_\gamma}\right)^2\frac{\Gamma_0^2}{\Gamma}, \quad (2)$$

TABLE I. Level lifetimes extracted for ^{112}Cd from the $(n, n'\gamma)$ reaction compared with those extracted with other methods, as tabulated in Ref. [35] for Coulomb excitation or recent (γ, γ') measurements.

Level (keV)	τ $(n, n'\gamma)$ (fs)	τ (Literature) (fs)	Method
1312.4	2200^{+3200}_{-800}	2900 ± 400	Coulex
1415.6	1000^{+1000}_{-340}	1300 ± 100	Coulex
1468.8	2000^{+4300}_{-800}	3900 ± 700	Coulex
2506.7	64 ± 12	53 ± 3	(γ, γ')
2829.2	39 ± 5	40 ± 4	(γ, γ')
2931.4	25 ± 6	17 ± 1	(γ, γ')
3131.3	39 ± 7	30 ± 1	(γ, γ')
3231.4	50 ± 6	38 ± 3	(γ, γ')
3301.0	150^{+180}_{-60}	93 ± 11	(γ, γ')
3375.4	75 ± 12	125 ± 19	(γ, γ')
3556.8	98 ± 40	750 ± 190	(γ, γ')
3568.0	89 ± 14	51 ± 13	(γ, γ')
3594.5	110 ± 20	221 ± 40	(γ, γ')
3682.8	46 ± 12	127 ± 20	(γ, γ')
3703.7	32 ± 6	94 ± 8	(γ, γ')
3810.0	14 ± 3	24 ± 5	(γ, γ')
3846.4	57 ± 13	285 ± 47	(γ, γ')
3868.9	19 ± 5	29 ± 7	(γ, γ')
3933.1	18 ± 6	109 ± 15	(γ, γ')

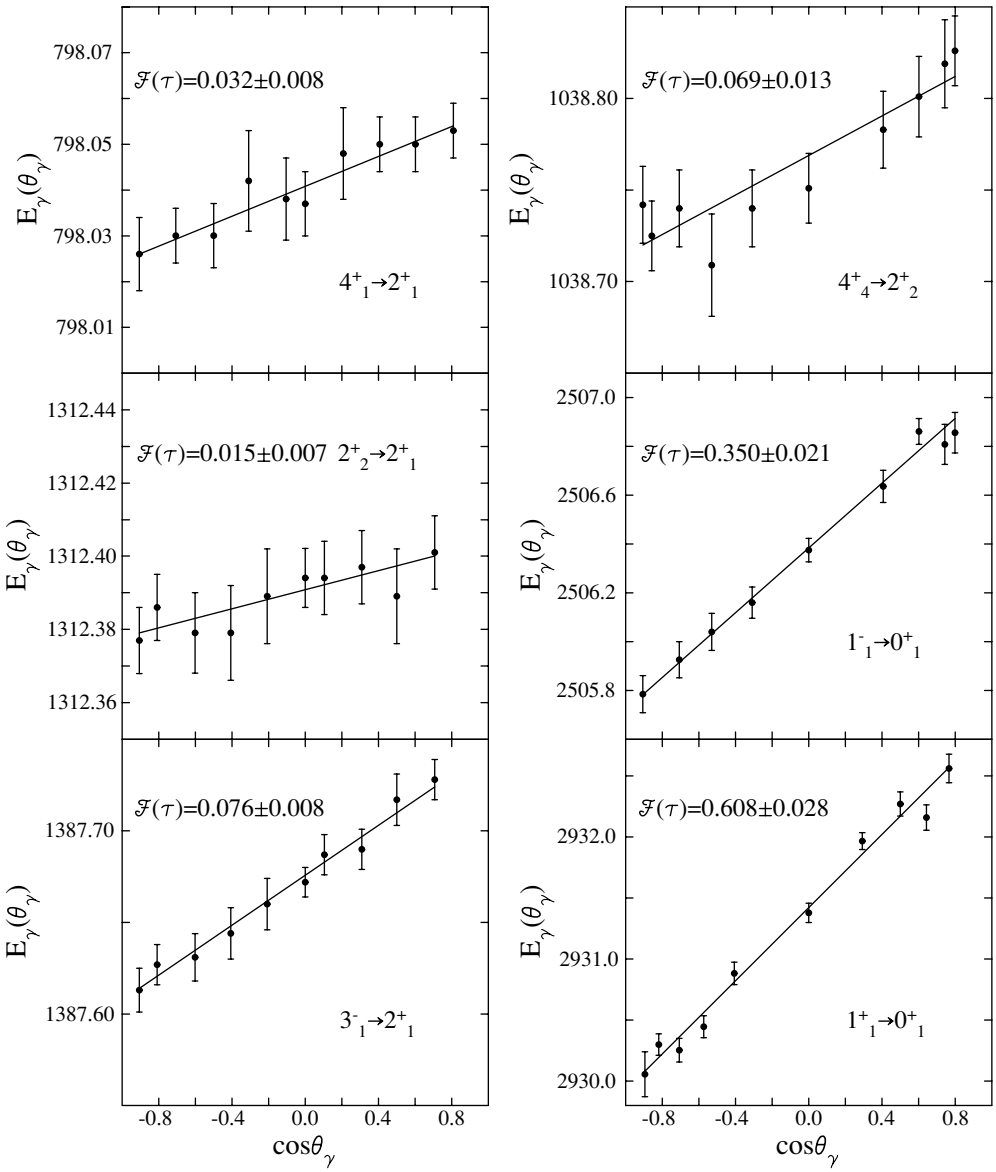

FIG. 1. Examples of Doppler shifts observed following the ^{112}Cd$(n, n'\gamma)$ reaction.

where g is the statistical spin factor $g = (2I_s + 1)/(2I_0 + 1) = 3$ in the present context, and Γ_0 and Γ denote the decay width to the ground state and the total decay width, respectively. The level lifetime can be deduced via

$$\tau_{(\gamma,\gamma')} = \frac{g(BR)^2\hbar}{I_{s,0}} \left(\pi \frac{\hbar c}{E_s}\right)^2, \qquad (3)$$

where the branching fraction BR for the state to decay to the ground state is $BR = \Gamma_0/\Gamma$. Hence, the comparison of (γ, γ') results with those from the $(n, n'\gamma)$ reaction rely on the *square* of the ground-state branching fraction implying that an accurate level and decay scheme must be in place. Two observations from an examination of Table I are immediate: there is remarkable agreement over two orders of magnitude for levels up to ≈3.4 MeV, whereas above 3.4 MeV the agreement becomes poor. For the low-lying states observed in Coulomb excitation, only the 1312-keV, 1415-keV, and 1468-keV levels have sufficiently short lifetimes to be measurable in the $(n, n'\gamma)$ reaction. While at the very limit of the technique (the 1312.4-keV γ ray has a forward-backward maximum shift of only 20 eV), the results are nonetheless significant and indicate that the technique remains valid down to relatively long lifetimes, and hence very low recoil velocities. At the other end of the measurement range, lifetimes at the few tens of fs compare well with those extracted from the results of (γ, γ') experiments [36]. In fact, below 3.4 MeV the only discrepancies occur for the 3231-keV ($\tau_{\gamma,\gamma'} = 38 \pm 3$ fs, $\tau_{n,n'\gamma} = 50 \pm 6$ fs) and 3375-keV ($\tau_{\gamma,\gamma'} = 125 \pm 19$ fs, $\tau_{n,n'\gamma} = 75 \pm 12$ fs) levels. Lifetimes extracted using the above procedure from the (γ, γ') work that are *longer* than those extracted using the $(n, n'\gamma)$ technique may indicate either an incomplete decay scheme for the particular level, and hence an incorrect (and larger) branching fraction BR is used, or an incorrect lifetime determination in the $(n, n'\gamma)$ study. This

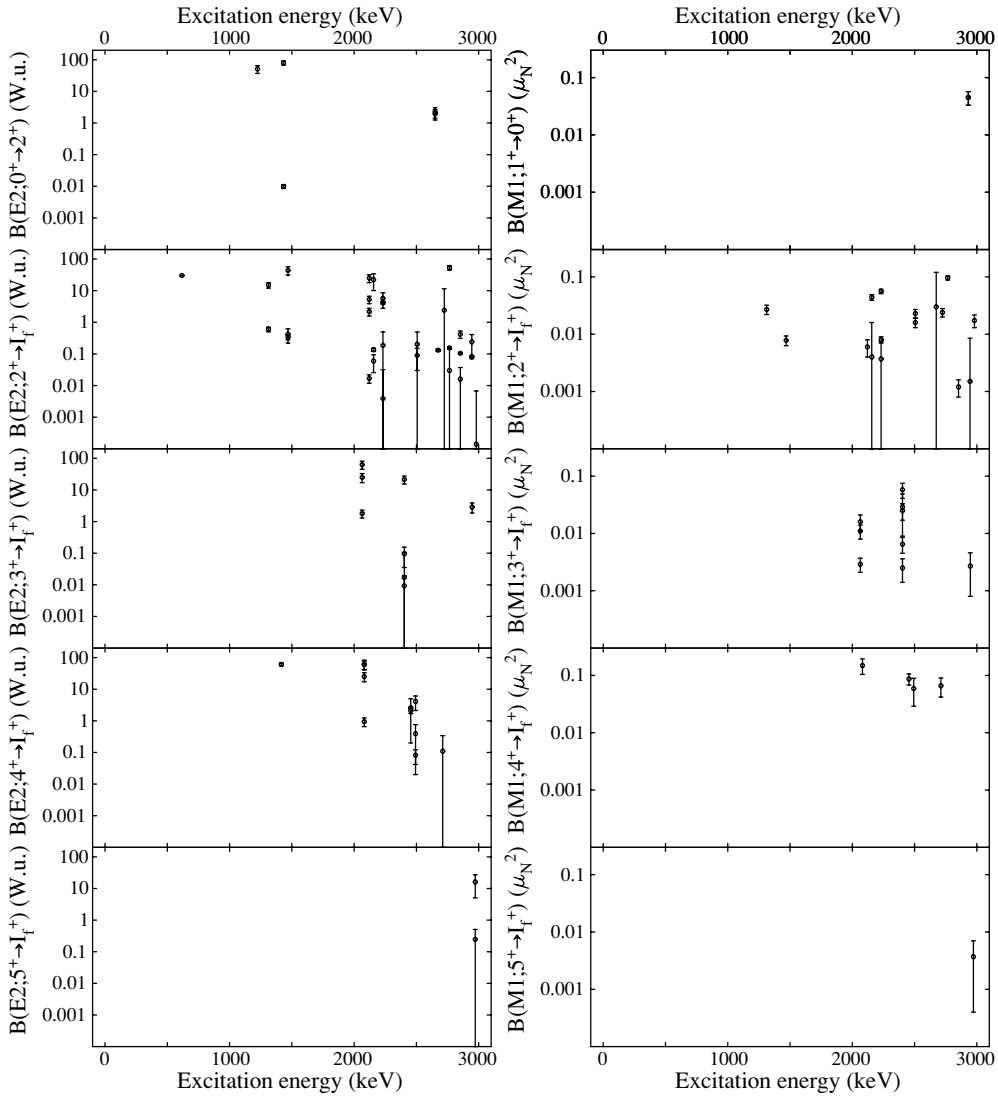

FIG. 2. Summary of $B(E2\downarrow)$ (left) and $B(M1\downarrow)$ (right) transition rates for positive-parity states below 3 MeV in ^{112}Cd. Upper limits on transition rates are not shown. Of note are the enhanced transitions, with $B(E2) > 5$ W.u. or $B(M1) > 0.01\ \mu_N^2$.

latter case becomes a possibility whenever the γ-ray spectrum became complex. While care has been taken to ensure that transitions used to extract the lifetimes are not members of doublets, the indicators for the presence of doublets (see Ref. [27] for a discussion) become weaker as the cross sections for individual levels become smaller, i.e., at higher excitation energy. Since a comprehensive ^{112}Cd level scheme is available below 3.4 MeV, the above discrepancies are likely due to the unplaced low-energy decay branches, i.e., an incorrect branching fraction BR. Above 3.4 MeV, the discrepancies can become quite large, approaching a factor of 8 for the 3556-keV level, and with factors of 2–3 common. This is not surprising since it is known that the level scheme is not complete above 3.4 MeV [27], and missing a 50% branch would result in an apparent (γ, γ') lifetime a factor of 4 times larger than in the $(n, n'\gamma)$ reaction.

Listed in Table II are the measured $F(\tau)$ values and the deduced lifetimes, along with the transition rates for individual transitions taking into account the level scheme as presented in Ref. [27]. While it is believed that the lifetimes are generally accurate, because of the limitations in the building of the decay scheme as highlighted by the vastly different lifetimes extracted compared with the (γ, γ') technique above 3.4 MeV, the transition rates above 3.4 MeV should be considered more as upper limits as they may be overestimated by factors of several, and perhaps as much as an order of magnitude. Figure 2 summarizes the results for the $B(E2)$ (left) and $B(M1)$ (right) transition rates for positive-parity levels below 3 MeV in excitation energy. Upper limits on transition rates are not included. Of interest are the enhanced transitions, namely those with a $B(E2)$ value above ≈ 5 W.u., or a $B(M1)$ value above $\approx 0.01\ \mu_N^2$.

IV. INTERPRETATIONS

The nucleus ^{112}Cd has been studied by a wide variety of probes that can be subdivided into selective and nonselective processes. Selective processes are those where the population

TABLE II. Results for lifetimes extracted for ^{112}Cd from the $(n, n'\gamma)$ reaction.

E_i (keV)	$F(\tau)$	τ (fs)	E_γ (keV)	E_f (keV)	$I_i^\pi \rightarrow I_f^\pi$	$B(E2; I_i^\pi \rightarrow I_f^\pi)$ (W.u.)	$B(M1; I_I^\pi \rightarrow I_f)$ (μ_N^2)	$B(E1; I_I^\pi \rightarrow I_f^\pi)$ (10^{-3} W.u.)
617.52			617.52	0.0	$2^+ \rightarrow 0_1^+$	30.2(3)[a]		
1224.41			606.84	617.5	$0^+ \rightarrow 2_1^+$	51(14)[a]		
1312.39	0.015(9)	2200^{+3200}_{-800}	1312.39	0.0	$2^+ \rightarrow 0_1^+$	0.6(1)[a]		
			694.84	617.5	$\rightarrow 2_1^+$	15(3)[a]	0.027(5)[a]	
1415.56	0.033(17)	1000^{+1000}_{-340}	798.04	617.5	$4^+ \rightarrow 2_1^+$	61(6)[a]		
1433.31			815.79	617.5	$0^+ \rightarrow 2_1^+$	0.0099(14)[a]		
			121.00	1312.4	$\rightarrow 2_2^+$	80(12)[a]		
1468.84	0.017(11)[a]	2000^{+4300}_{-800}	1468.84	0.0	$2^+ \rightarrow 0_1^+$	0.34(6)[a]		
			851.27	617.5	$\rightarrow 2_1^+$	0.12(7)	$0.0147^{+0.0032}_{-0.0022}$[a]	
			244.80	1224.4	$\rightarrow 0_2^+$	$44.6^{+9.8}_{-6.8}$[a]		
2005.19	0.083(1)	380(65)	1387.68	617.5	$3^- \rightarrow 2_1^+$			0.335(57)
			692.79	1312.4	$\rightarrow 2_2^+$			0.60(10)
			536.31	1468.8	$\rightarrow 2_3^+$			0.065(13)
2064.51	0.053(11)	680(190)	1447.00	617.5	$3^+ \rightarrow 2_1^+$	1.8(5)	0.0029(8)	
			752.14	1312.4	$\rightarrow 2_2^+$	63(18)	0.011(3)	
			648.91	1415.6	$\rightarrow 4_1^+$	25(8)	0.016(5)	
2081.72	0.065(18)	500(150)	1464.04	617.5	$4^+ \rightarrow 2_1^+$	0.95(29)		
			769.36	1312.4	$\rightarrow 2_2^+$	60(18)		
			666.15	1415.6	$\rightarrow 4_1^+$	25(8)	0.149(45)	
			612.88	1468.8	$\rightarrow 2_3^+$	61(21)		
2121.53	0.042(11)	740(200)	2121.49	0.0	$2^+ \rightarrow 0_1^+$	0.017(5)		
			1504.04	617.5	$\rightarrow 2_1^+$	2.2(6)	$0.0060^{+0.0022}_{-0.0013}$	
			897.07	1224.5	$\rightarrow 0_2^+$	5.3(14)		
			808.82	1312.4	$\rightarrow 2_2^+$	<2.8	<0.004	
			688.23	1433.1	$\rightarrow 0_3^+$	25(7)		
2156.18	0.100(11)	310(35)	2156.20	0.0	$2^+ \rightarrow 0_1^+$	0.136(16)		
			1538.65	617.5	$\rightarrow 2_1^+$	$0.060^{+0.027}_{-0.040}$	0.044(5)	
			687.41	1468.8	$\rightarrow 2_3^+$	22^{+6}_{-19}	$0.004^{+0.020}_{-0.004}$	
2231.20	0.138(12)	220(20)	1613.66	617.5	$2^+ \rightarrow 2_1^+$	$0.004^{+0.018}_{-0.004}$	0.056(5)	
			1006.81	1224.5	$\rightarrow 0_2^+$	4.14(39)		
			918.72	1312.4	$\rightarrow 2_2^+$	$0.19^{+0.46}_{-0.16}$	$0.0080^{+0.0012}_{-0.0008}$	
			762.41	1468.8	$\rightarrow 2_3^+$	$5.7^{+2.6}_{-3.2}$	$0.0037^{+0.0041}_{-0.0033}$	
2300.74		>900	1683.22	617.5	$0^+ \rightarrow 2_1^+$	<1.4		
			831.79	1468.8	$\rightarrow 2_3^+$	<23		
2373.28	0.055(32)	590^{+880}_{-230}	957.72	1415.6	$5^- \rightarrow 4_1^+$			$0.79^{+0.51}_{-0.47}$
			367.90	2005.2	$\rightarrow 3_1^-$	58^{+39}_{-37}		
			291.50	2081.7	$\rightarrow 4_3^+$			$0.32^{+0.21}_{-0.20}$
2403.03	0.092(26)	340^{+150}_{-80}	1785.48	617.5	$3^+ \rightarrow 2_1^+$	$0.011^{+0.010}_{-0.007}$	0.0065(20)	
			1090.56	1312.4	$\rightarrow 2_2^+$	0.09(6)	0.025(8)	
			987.89	1415.6	$\rightarrow 4_1^+$	$0.017^{+0.090}_{-0.017}$	0.058(17)	
			934.19	1468.8	$\rightarrow 2_3^+$	21(6)	$0.0025^{+0.0012}_{-0.0009}$	
			531.89	1870.7	$\rightarrow 4_2^+$	16^{+40}_{-15}	$0.029^{+0.013}_{-0.027}$	
2416.00	0.137(28)	220(50)	1798.50	615.7	$3^- \rightarrow 2_1^+$			0.194(44)
			1103.58	1312.4	$\rightarrow 2_2^+$			0.395(90)
			946.92	1468.8	$\rightarrow 2_3^+$			0.126(33)
			411.39	2005.2	$\rightarrow 3_1^-$	85^{+115}_{-62}	0.25(8)	
2454.52	0.069(13)	500^{+130}_{-80}	1142.21	1312.4	$4^+ \rightarrow 2_2^+$	$2.1^{+0.3}_{-0.5}$		
			1038.93	1415.6	$\rightarrow 4_1^+$	$2.6^{+4.0}_{-2.4}$	$0.087^{+0.018}_{-0.020}$	

TABLE II. *(Continued.)*

E_i (keV)	$F(\tau)$	τ (fs)	E_γ (keV)	E_f (keV)	$I_i^\pi \rightarrow I_f^\pi$	$B(E2; I_i^\pi \rightarrow I_f^\pi)$ (W.u.)	$B(M1; I_i^\pi \rightarrow I_f)$ (μ_N^2)	$B(E1; I_i^\pi \rightarrow I_f^\pi)$ (10^{-3} W.u.)
2493.16	0.055(26)	630^{+610}_{-210}	1875.70	617.5	$4^+ \rightarrow 2_1^+$	0.08(4)		
			1077.60	1415.6	$\rightarrow 4_1^+$	$0.39^{+0.47}_{-0.31}$	0.059(30)	
			1024.29	1468.8	$\rightarrow 2_3^+$	4.1(20)		
2506.33	0.109(15)	300(45)	1888.79	617.5	$2^+ \rightarrow 2_1^+$	$0.09^{+0.07}_{-0.05}$	0.023(4)	
			1194.00	1312.4	$\rightarrow 2_2^+$	$0.20^{+0.41}_{-0.17}$	0.016(3)	
2506.73	0.374(42)	64(12)	2506.70	0.0	$1^- \rightarrow 0_1^+$			0.356(67)
			1282.29	1224.4	$\rightarrow 0_2^+$			0.146(30)
			1073.32	1433.3	$\rightarrow 0_3^+$			0.218(46)
			1037.82	1468.8	$\rightarrow 2_3^+$			0.340(73)
2570.29		>1000	1154.75	1415.5	$5^- \rightarrow 4_1^+$			<0.09
			699.59	1870.8	$\rightarrow 4_2^+$			<0.3
			565.10	2005.2	$\rightarrow 3_1^-$	<46	<0.03	
			197.03	2373.3	$\rightarrow 5_1^-$	[b]	[b]	
2591.05		>1000	1175.50	1415.5	$4^- \rightarrow 4_1^+$			<0.1
			720.44	1870.8	$\rightarrow 4_2^+$			<0.08
			585.78	2005.2	$\rightarrow 3_1^-$	<50	<0.03	
			526.52	2064.5	$\rightarrow 3_1^+$			<0.8
2635.00		>1000	2017.50	617.5	$3^+ \rightarrow 2_1^+$	<0.04	<0.0004	
			1322.59	1312.4	$\rightarrow 2_2^+$	<1.3	<0.005	
			1219.40	1415.6	$\rightarrow 4_1^+$	[c]	[c]	
			629.80	2005.2	$\rightarrow 3_1^-$			<0.4
			570.50	2064.5	$\rightarrow 3_1^+$	<26	<0.02	
2650.16	0.100(33)	330^{+180}_{-90}	2032.62	617.5	$0^+ \rightarrow 2_1^+$	1.9(7)		
			1337.75	1312.4	$\rightarrow 2_2^+$	2.2(8)		
2665.61		>300	1250.17	1415.5	$5^+ \rightarrow 4_1^+$	<0.1	<0.024	
			795.08	1870.7	$\rightarrow 4_2^+$	<0.8	<0.06	
			601.01	2064.5	$\rightarrow 3_1^+$	<250		
			583.92	2081.7	$\rightarrow 4_3^+$	<40	<0.3	
2668.93	0.105(13)	310(45)	2051.50	617.5	$2^- \rightarrow 2_1^+$			0.0226(34)
			1356.52	1312.4	$\rightarrow 2_2^+$			0.436(63)
			663.59	2005.2	$\rightarrow 3_1^-$	21^{+10}_{-15}	$0.012^{+0.014}_{-0.010}$	
2674.02	0.435(19)	50(4)	2056.48	617.5	$2^+ \rightarrow 2_1^+$	0.131(10)	$0.03^{+0.16}_{-0.02}$	
2711.29	0.092(31)	370^{+210}_{-100}	1295.74	1415.5	$4^+ \rightarrow 4_1^+$	$0.11^{+0.23}_{-0.11}$	0.066(24)	
			705.95	2005.2	$\rightarrow 3_1^-$			0.190(75)
2723.88	0.139(20)	230(35)	2106.31	617.5	$2^+ \rightarrow 2_1^+$	$2.4^{+9.1}_{-2.4}$	0.024(4)	
			718.89	2005.2	$\rightarrow 3_1^-$			0.506(81)
2765.75	0.440(22)	49(4)	2765.70	0.0	$2^+ \rightarrow 0_1^+$	0.155(14)		
			2148.21	617.5	$\rightarrow 2_1^+$	$0.03^{+0.12}_{-0.03}$	0.096(8)	
			1453.40	1312.4	$\rightarrow 2_2^+$	5.8(3)		
			1296.90	1468.8	$\rightarrow 2_3^+$	[c]	[c]	
			895.00	1871.2	$\rightarrow 0_4^+$	53(9)		
2773.18		>1000	1460.83	1312.4	$0^+ \rightarrow 2_2^+$	<3		
			541.80	2231.2	$\rightarrow 2_6^+$	<90		
2791.80		>140	786.59	2005.2	$4^- \rightarrow 3_1^-$	<4	<0.8	
2816.90		>600	1401.30	1415.6	$4^+ \rightarrow 4_1^+$	[c]	[c]	
			811.30	2005.2	$\rightarrow 3_1^-$			[c]
			734.90	2081.7	$\rightarrow 4_3^+$	[c]	[c]	
2829.22	0.498(33)	39(5)	2829.20	0.0	$1^- \rightarrow 0_1^+$			0.209(27)
			2211.65	617.5	$\rightarrow 2_1^+$			0.557(72)
			957.40	1871.2	$\rightarrow 0_4^+$			[c]

TABLE II. *(Continued.)*

E_i (keV)	$F(\tau)$	τ (fs)	E_γ (keV)	E_f (keV)	$I_i^\pi \to I_f^\pi$	$B(E2; I_i^\pi \to I_f^\pi)$ (W.u.)	$B(M1; I_i^\pi \to I_f)$ (μ_N^2)	$B(E1; I_i^\pi \to I_f^\pi)$ (10^{-3} W.u.)
2834.26		>500	2216.75	617.5	$0^+ \to 2_1^+$	<0.7		
			1521.82	1312.4	$\to 2_2^+$	<1.1		
			712.68	2121.5	$\to 2_4^+$	<40		
2840.29		>700	1424.73	1415.5	$4^+ \to 4_1^+$	<4	<0.013	
2852.92	0.060(17)	640^{+300}_{-150}	2852.87	0.0	$2^+ \to 0_1^+$	0.105(4)		
			2235.46	617.5	$\to 2_1^+$	$0.016^{+0.021}_{-0.012}$	0.0012(4)	
			1540.40	1312.4	$\to 2_2^+$	<1.7	<0.008	
			1419.60	1433.3	$\to 0_3^+$	$0.42^{+0.08}_{-0.14}$		
2866.86	0.043(25)	800^{+1100}_{-300}	1451.30	1415.6	$3^- \to 4_1^+$			$0.061^{+0.039}_{-0.036}$
			861.68	2005.2	$\to 3_1^-$	$0.18^{+0.73}_{-0.20}$	0.061(38)	
			784.91	2081.7	$\to 4_3^+$			$0.110^{+0.070}_{-0.065}$
			450.75	2416.0	$\to 3_2^-$	<100	0.046(37)	
2867.48	0.236(97)	130^{+110}_{-50}	2249.91	617.5	$3^+ \to 2_1^+$	<5.4	<0.04	
			1555.10	1312.4	$\to 2_2^+$	[c]	[c]	
			1398.64	1468.8	$\to 2_3^+$	[c]	[c]	
2882.70		>1000	1570.51	1312.4	$0^+ \to 2_2^+$	<0.46		
			1413.86	1468.8	$\to 2_3^+$	<2.7		
			726.79	2156.1	$\to 2_5^+$	<28		
2893.62		>600	2276.07	617.5	$4^+ \to 2_1^+$	<0.5		
			811.90	2081.7	$\to 4_3^+$	[c]	[c]	
			771.76	2121.2	$\to 2_4^+$	<42		
2899.09	0.164(35)	190(50)	1483.53	1415.5	$5^- \to 4_1^+$			0.68(18)
2924.83		>200	1509.36	1415.5	$4^- \to 4_1^+$			
			1054.24	1870.8	$\to 4_2^+$			
			919.58	2005.2	$\to 3_1^-$			
			551.63	2373.3	$\to 5_1^-$			
			333.72	2591.0	$\to 4_1^-$			
2931.51	0.608(63)	25(6)	2931.42	0.0	$1^+ \to 0_1^+$		0.045(12)	
			2314.12	617.5	$\to 2_1^+$	<4	<0.06	
			1618.84	1312.4	$\to 2_2^+$	<28	<0.15	
2944.86	0.061(26)	590^{+460}_{-190}	2944.78	0.0	$2^+ \to 0_1^+$	0.082(4)		
			2327.44	617.5	$\to 2_1^+$	$0.24^{+0.09}_{-0.24}$	$0.0015^{+0.0030}_{-0.0011}$	
2947.76	0.238(47)	120(35)	2330.22	617.5	$3^+ \to 2_1^+$	$2.9^{+1.0}_{-0.7}$	$0.0027^{+0.0023}_{-0.0015}$	
2969.84			1554.28	1415.5	$5^+ \to 4_1^+$			
2972.48	0.042(28)	830^{+1600}_{-340}	1556.80	1415.5	$5^+ \to 4_1^+$	<3.5	<0.02	
			890.77	2081.7	$\to 3_2^+$	$0.25^{+0.26}_{-0.18}$	0.015(10)	
			804.89	2167.7	$\to 6_1^+$	16(11)	$0.0037^{+0.0037}_{-0.0031}$	
2980.82	0.156(31)	200(50)	2363.27	617.5	$2^+ \to 2_1^+$	$0.0001^{+0.0066}_{-0.0001}$	0.0173(43)	
			1668.40	1312.4	$\to 2_2^+$	<1	<0.006	
			1512.13	1468.8	$\to 2_3^+$	<2.5	<0.013	
3002.13	0.116(42)	280^{+180}_{-80}	2384.54	617.5	$(3^+) \to 2_1^+$	0.54(21)	0.00010(8)	
			1689.70	1312.4	$\to 2_2^+$	[c]	[c]	
			1586.57	1415.5	$\to 4_1^+$	$0.047^{+0.060}_{-0.040}$	0.018(7)	
			996.75	2005.2	$\to 3_1^-$			0.26(11)
3048.95	0.24(12)	120^{+180}_{-50}	1633.39	1415.5	$2\text{–}6 \to 4_1^+$			
			967.63	2081.7	$\to 4_3^+$			
3066.31		>300	2448.76	617.5	$3^- \to 2_1^+$			<0.06
			1753.80	1312.4	$\to 2_2^+$			<0.09

TABLE II. *(Continued.)*

E_i (keV)	$F(\tau)$	τ (fs)	E_γ (keV)	E_f (keV)	$I_i^\pi \rightarrow I_f^\pi$	$B(E2; I_i^\pi \rightarrow I_f^\pi)$ (W.u.)	$B(M1; I_i^\pi \rightarrow I_f)$ (μ_N^2)	$B(E1; I_i^\pi \rightarrow I_f^\pi)$ (10^{-3} W.u.)
3068.68		>800	1756.30	1312.4	$4^+ \rightarrow 2_2^+$	<0.27		
			1653.09	1415.6	$\rightarrow 4_1^+$	<0.14	<0.002	
			1599.70	1468.8	$\rightarrow 2_3^+$	<1		
			1063.49	2005.2	$\rightarrow 3_1^-$	<0.26		<0.16
3071.49		>360	1066.28	2005.2	$3,4 \rightarrow 3_1^-$			
			1006.90	2064.5	$\rightarrow 3_1^+$			
3075.27	0.081(51)	410^{+770}_{-170}	1659.70	1415.5	$5^+ \rightarrow 4_1^+$	$0.08^{+0.09}_{-0.07}$	0.030(20)	
3102.15	0.579(62)	30(8)	3102.10	0.0	$1 \rightarrow 0_1^+$			
3105.61	0.079(49)	450^{+780}_{-190}	2488.14	617.5	$2,3 \rightarrow 2_1^+$			
			1792.77	1312.4	$\rightarrow 2_2^+$			
			1690.10	1415.5	$\rightarrow 4_1^+$			
3109.82	0.170(51)	190^{+90}_{-50}	3110.01	0.0	$1 \rightarrow 0_1^+$			
			2492.24	617.5	$\rightarrow 2_1^+$			
			1641.14	1468.9	$\rightarrow 2_3^+$			
3133.26	0.513(43)	39(7)	3133.21	0.0	$1 \rightarrow 0_1^+$			
3135.84	0.075(32)	480^{+390}_{-160}	2518.43	617.5	$2,3 \rightarrow 2_1^+$			
			1823.39	1312.4	$\rightarrow 2_2^+$			
			1667.00	1468.9	$\rightarrow 2_3^+$			
			1071.26	2064.5	$\rightarrow 3_1^+$			
3145.39	0.171(41)	190^{+70}_{-40}	1729.82	1415.6	$4^+ \rightarrow 4_1^+$	1.4(7)	0.049(11)	
			1063.60	2081.8	$\rightarrow 4_3^+$	[c]	[c]	
3163.03	0.093(28)	370^{+180}_{-100}	3162.98	0.0	$2^+ \rightarrow 0_1^+$	0.22(8)		
			656.30	2506.7	$\rightarrow 1_1^-$			[c]
3169.56	0.156(14)	210(20)	2552.01	617.5	$2^+ \rightarrow 2_1^+$	$0.20^{+0.08}_{-0.06}$	0.006(1)	
			1945.14	1224.5	$\rightarrow 0_2^+$	1.8(2)		
			1164.20	2005.3	$\rightarrow 3_1^-$			[c]
3178.80	0.202(32)	150(35)	3178.76	0.0	$2^+ \rightarrow 0_1^+$	0.14(3)		
			2561.23	617.5	$\rightarrow 2_1^+$	<1.4	<0.02	
3189.87		>510	1774.30	1415.6	$4\text{–}6 \rightarrow 4_1^+$			
			1022.10	2167.7	$\rightarrow 6_1^+$			
3190.06	0.561(16)	32(2)	2572.51	617.5	$2,(3) \rightarrow 2_1^+$			
3194.50	0.203(60)	150(60)	2576.72	617.5	$2^+, (3^+) \rightarrow 2_1^+$			
			1882.10	1312.4	$\rightarrow 2_2^+$			
			1189.41	2005.3	$\rightarrow 3_1^-$			
3201.42	0.048(22)	760^{+680}_{-250}	1785.80	1415.6	$5^- \rightarrow 4_1^+$			[c]
			1196.21	2005.3	$\rightarrow 3_1^-$	<20		
3203.26	0.176(65)	180^{+130}_{-60}	2585.70	617.5	$3^{(+)} \rightarrow 2_1^+$	0.018(6)	$0.012^{+0.019}_{-0.010}$	
3205.75		>160	1790.20	1415.6	$2\text{–}4 \rightarrow 4_1^+$			
			1736.90	1468.8	$\rightarrow 2_3^+$			
3206.45	0.270(57)	110(35)	2588.85	617.5	$2\text{–}4 \rightarrow 2_1^+$			
			1084.93	2121.5	$\rightarrow 2_4^+$			
3206.71	0.065(27)	550^{+400}_{-170}	1894.30	1312.4	$2\text{–}4 \rightarrow 2_2^+$			
			1792.10	1415.6	$\rightarrow 4_1^+$			
3231.41	0.446(27)	50(6)	3231.35	0.0	$1^+ \rightarrow 0_1^+$		<0.027	
			2614.02	617.5	$\rightarrow 2_1^+$	<1.3	<0.02	
			1919.40	1312.4	$\rightarrow 2_2^+$	[c]	[c]	
3242.59	0.111(63)	310^{+450}_{-120}	3242.49	0.0	$2^+ \rightarrow 0_1^+$	0.056(34)		
			2625.07	617.5	$\rightarrow 2_1^+$	0.19(13)	$0.0008^{+0.0010}_{-0.0006}$	
			1161.08	2081.7	$\rightarrow 4_3^+$	15(10)		

TABLE II. *(Continued.)*

E_i (keV)	$F(\tau)$	τ (fs)	E_γ (keV)	E_f (keV)	$I_i^\pi \to I_f^\pi$	$B(E2; I_i^\pi \to I_f^\pi)$ (W.u.)	$B(M1; I_I^\pi \to I_f)$ (μ_N^2)	$B(E1; I_I^\pi \to I_f^\pi)$ (10^{-3} W.u.)
3246.88	0.142(23)	230(45)	2629.34	617.5	$2,3 \to 2_1^+$			
			1778.00	1468.9	$\to 2_3^+$			
3251.86	0.132(98)	250^{+840}_{-120}	2634.31	617.5	$0^+ \to 2_1^+$	$0.80^{+0.74}_{-0.62}$		
3254.18	0.099(75)	350^{+1200}_{-170}	2636.62	617.5	$2\text{–}4 \to 2_1^+$			
			1942.01	1312.4	$\to 2_2^+$			
3254.46	0.324(65)	82(25)	1838.89	1415.6	$4^+ \to 4_1^+$	$4.9^{+1.6}_{-1.3}$	$0.0038^{+0.0044}_{-0.0029}$	
			1248.14	2005.3	$\to 3_1^-$			1.67(51)
3266.61	0.126(29)	270(75)	1851.04	1415.6	$3,4,5 \to 4_1^+$			
3269.49	0.136(71)	250^{+310}_{-100}	1854.04	1415.6	$4 \to 4_1^+$			
			1264.25	2005.3	$\to 3_1^-$			
3291.16	0.097(63)	360^{+730}_{-160}	1875.70	1415.6	$\to 4_1^+$			
			1285.95	2005.3	$\to 3_1^-$			
			1209.40	2081.7	$\to 4_3^+$			
3297.01	0.065(24)	550^{+340}_{-160}	2679.46	617.5	$3 \to 2_1^+$			
			1881.50	1415.6	$\to 4_1^+$			
3300.99	0.21(10)	150^{+180}_{-60}	3300.94	0.0	$1 \to 0_1^+$			
3303.34	0.136(15)	250(35)	2685.78	617.5	$2,3 \to 2_1^+$			
3312.19	0.265(42)	110(25)	2694.56	617.5	$1,2,3 \to 2_1^+$			
			2000.01	1312.4	$\to 2_2^+$			
			1306.97	2005.3	$\to 3_1^-$			
3319.88	0.133(24)	250(40)	2702.24	617.5	$\to 2_1^+$			
			1851.04	1468.9	$\to 2_3^+$			
3332.05	0.179(37)	180(45)	1916.72	1415.6	$3,4,5 \to 4_1^+$			
			1326.83	2005.3	$\to 3_1^-$			
3332.47	0.213(35)	140(35)	2714.91	617.5	$1,2,3 \to 2_1^+$			
3336.03	0.205(44)	150(40)	2718.48	617.5	$2,3 \to 2_1^+$			
3341.86	0.430(25)	53(6)	2724.31	617.5	$3^+ \to 2_1^+$	3.14(33)	$0.00095^{+0.00059}_{-0.00033}$	
3353.37	0.167(39)	190(55)	2735.81	617.5	$1,2,3 \to 2_1^+$			
3363.59	0.102(29)	340^{+150}_{-80}	3363.67	0.0	$2^+ \to 0_1^+$	0.064(20)		
			2745.86	617.5	$\to 2_1^+$	$0.058^{+0.038}_{-0.033}$	0.0041(11)	
3364.01	0.15(12)	220^{+1000}_{-110}	909.48	2454.4	$\to 4_4^+$			
3369.63	0.441(21)	50(5)	2752.08	617.5	$2,3 \to 2_1^+$			
			1900.77	1468.9	$\to 2_3^+$			
3375.47	0.326(32)	75(12)	3375.40	0.0	$1 \to 0_1^+$			
			2758.02	617.5	$\to 2_1^+$			
3378.49	0.061(25)	590^{+440}_{-180}	2761.18	617.5	$\to 2_1^+$			
			1909.63	1468.9	$2,3,4 \to 2_3^+$			
3383.61	0.218(29)	140(25)	2766.05	617.5	$1,2,3 \to 2_1^+$			
			1227.70	2156.2	$\to 2_5^+$			
3392.77		>1000	3392.72	0.0	$1 \to 0_1^+$			
3393.39	0.002	>1400	2775.83	617.5	$1,2,3 \to 2_1^+$			
3393.63	0.133(83)	250^{+470}_{-110}	977.59	2416.2	$\to 3_2^-$			
3402.93		>760	2785.37	617.5	$3^+ \to 2_1^+$	<0.16	<0.001	
3425.61	0.215(49)	140(40)	2113.19	1312.4	$\to 2_2^+$			
3426.32	0.46(10)	47^{+24}_{-15}	2808.76	617.5	$\to 2_1^+$			
3428.77	0.251(83)	120^{+70}_{-40}	3428.71	0.0	$2^+ \to 0_1^+$	$0.056^{+0.029}_{-0.021}$		
			2811.20	617.5	$\to 2_1^+$	$1.06^{+0.53}_{-0.39}$	0.018(6)	

TABLE II. *(Continued.)*

E_i (keV)	$F(\tau)$	τ (fs)	E_γ (keV)	E_f (keV)	$I_i^\pi \rightarrow I_f^\pi$	$B(E2; I_i^\pi \rightarrow I_f^\pi)$ (W.u.)	$B(M1; I_I^\pi \rightarrow I_f)$ (μ_N^2)	$B(E1; I_I^\pi \rightarrow I_f^\pi)$ (10^{-3} W.u.)
3433.80	0.200(64)	160^{+90}_{-50}	2018.23	1415.2	3–5 $\rightarrow 4_1^+$			
3452.89	0.108(68)	320^{+600}_{-140}	2835.33	617.5	3^+,(2) $\rightarrow 2_1^+$			
			2037.39	1415.2	$\rightarrow 4_1^+$			
3455.40	0.083(44)	420^{+500}_{-160}	2837.85	617.5	2,3 $\rightarrow 2_1^+$			
3478.47	0.097(69)	360^{+980}_{-160}	2861.00	617.5	1–3 $\rightarrow 2_1^+$			
			2166.06	1312.4	$\rightarrow 2_2^+$			
3487.55	0.253(36)	120(25)	2869.99	617.5	$3^+ \rightarrow 2_1^+$	<1.3	<0.02	
3489.93	0.287(40)	98(19)	2872.40	617.5	3,5 $\rightarrow 2_1^+$			
			2074.36	1415.2	$\rightarrow 4_1^+$			
			1368.12	2121.5	$\rightarrow 2_4^+$			
3500.41	0.150(25)	220(45)	2882.85	617.5	2,3 $\rightarrow 2_1^+$			
3511.67		>700	1138.40	2373.2	$\rightarrow 5_1^-$			
3512.79	0.205(51)	150(50)	2895.23	617.5	$3^+ \rightarrow 2_1^+$	$0.026^{+0.021}_{-0.016}$	0.015(4)	
3522.51	0.457(22)	48(4)	2904.95	617.5	1–3 $\rightarrow 2_1^+$			
3531.33	0.266(58)	110(35)	2913.77	617.5	$3^+ \rightarrow 2_1^+$	<0.076	<0.026	
			2218.90	1312.4	$\rightarrow 2_2^+$			
3540.28	0.658(26)	22(3)	2922.72	617.5	1–3 $\rightarrow 2_1^+$			
3556.84	0.367(19)	69(6)	2939.77	617.5	1–3 $\rightarrow 2_1^+$			
3557.33	0.274(78)	98(40)	3556.78	0.0	$1 \rightarrow 0_1^+$			
3568.06	0.306(32)	89(14)	3568.00	0.0	$2^+ \rightarrow 0_1^+$	0.138(22)		
			2950.52	617.5	$\rightarrow 2_1^+$	$0.32^{+0.09}_{-0.16}$	$0.0024^{+0.0029}_{-0.0015}$	
			2099.17	1468.9	$\rightarrow 2_3^+$	$0.0003^{+0.2}_{-0.0003}$	0.026(4)	
3574.52	0.21(14)	140^{+340}_{-70}	2956.96	617.5	2,3 $\rightarrow 2_1^+$			
3579.25	0.167(35)	190(50)	2961.69	617.5	2,3 $\rightarrow 2_1^+$			
3594.59	0.257(35)	110(20)	3594.49	0.0	$1 \rightarrow 0_1^+$			
			2977.24	617.5	$\rightarrow 2_1^+$			
3598.81	0.473(65)	45(12)	2981.25	617.5	$3^+ \rightarrow 2_1^+$	$0.060^{+0.094}_{-0.047}$	0.047(10)	
3608.87	0.181(33)	180(40)	2991.30	617.5	$\rightarrow 2_1^+$			
3613.41	0.215(72)	140^{+90}_{-40}	2995.85	617.5	$3^+ \rightarrow 2_1^+$	$0.31^{+0.17}_{-0.26}$	$0.0016^{+0.0047}_{-0.0012}$	
			2143.97	1468.9	$\rightarrow 2_3^+$			
3618.40	0.33(15)	80^{+90}_{-35}	3000.83	617.5	$\rightarrow 2_1^+$			
3622.18	0.456(71)	48(14)	3004.62	617.5	$\rightarrow 2_1^+$			
3646.44	0.098(23)	350^{+120}_{-70}	3028.88	617.5	1–3 $\rightarrow 2_1^+$			
3652.16	0.178(41)	180(55)	3652.07	0.0	$1 \rightarrow 0_1^+$			
			3034.60	617.5	1–3 $\rightarrow 2_1^+$			
3665.78	0.169(26)	190(35)	3048.22	617.5	3,(2) $\rightarrow 2_1^+$			
3676.56	0.232(61)	130(45)	3059.00	617.5	2,3 $\rightarrow 2_1^+$			
3682.82	0.468(66)	46(12)	3682.76	0.0	$\rightarrow 0_1^+$			
3687.92	0.173(50)	190(70)	3687.86	0.0	$1 \rightarrow 0_1^+$			
3690.68	0.21(10)	140^{+160}_{-60}	3073.12	617.5	2,3 $\rightarrow 2_1^+$			
3697.69	0.095(75)	370^{+1500}_{-180}	3080.13	617.5	$2^+ \rightarrow 2_1^+$	$0.25^{+0.24}_{-0.20}$		
3703.81	0.564(47)	32(6)	3703.74	0.0	$1 \rightarrow 0_1^+$			
3707.39	0.435(56)	52(12)	3089.83	617.5	$\rightarrow 2_1^+$			
3722.70	0.65(14)	23^{+17}_{-11}	3105.13	617.5	$\rightarrow 2_1^+$			
3731.95	0.174(66)	180^{+130}_{-60}	3114.39	617.5	1–3 $\rightarrow 2_1^+$			
3739.56	0.293(61)	95(29)	3121.99	617.5	$3^+ \rightarrow 2_1^+$	$0.084^{+0.112}_{-0.060}$	0.018(5)	
3743.78	0.337(32)	78(11)	3126.22	617.5	$3^+ \rightarrow 2_1^+$	1.08(16)	$0.00016^{+0.00020}_{-0.00014}$	
3754.10		>600	2338.58	1415.2	$\rightarrow 4_1^+$			

TABLE II. *(Continued.)*

E_i (keV)	$F(\tau)$	τ (fs)	E_γ (keV)	E_f (keV)	$I_i^\pi \rightarrow I_f^\pi$	$B(E2; I_i^\pi \rightarrow I_f^\pi)$ (W.u.)	$B(M1; I_I^\pi \rightarrow I_f)$ (μ_N^2)	$B(E1; I_I^\pi \rightarrow I_f^\pi)$ (10^{-3} W.u.)
3755.46	0.498(79)	41(13)	3755.39	0.0	$1 \rightarrow 0_1^+$			
3763.94	0.203(20)	150(20)	3146.38	617.5	$1\text{–}3 \rightarrow 2_1^+$			
3770.47	0.517(58)	38(9)	3152.90	617.5	$2,3 \rightarrow 2_1^+$			
3783.20	0.119(78)	290^{+620}_{-130}	3165.63	617.5	$3^+ \rightarrow 2_1^+$	$0.24^{+0.20}_{-0.17}$	$0.00075^{+0.00091}_{-0.00052}$	
3804.87	0.121(83)	280^{+690}_{-130}	3187.30	617.5	$1\text{–}3 \rightarrow 2_1^+$			
3810.04	0.748(35)	14(3)	3809.97	0.0	$1 \rightarrow 0_1^+$			
3810.88	0.286(71)	98^{+44}_{-26}	3193.31	617.5	$1\text{–}3 \rightarrow 2_1^+$			
3832.66	0.559(75)	32(10)	3215.09	617.5	$1\text{–}3 \rightarrow 2_1^+$			
3844.25	0.031	>380	3226.68	617.5	$\rightarrow 2_1^+$			
3846.48	0.413(55)	57(13)	3846.41	0.0	$1 \rightarrow 0_1^+$			
3869.00	0.692(52)	19(5)	3868.93	0.0	$1 \rightarrow 0_1^+$			
3878.62	0.34(10)	76(35)	3261.05	617.5	$2,3 \rightarrow 2_1^+$			
3929.22	0.16(13)	200^{+1200}_{-110}	3311.64	617.5	$\rightarrow 2_1^+$			
3932.19	0.226(74)	130^{+80}_{-40}	3314.61	617.5	$\rightarrow 2_1^+$			
3933.08	0.696(70)	18(6)	3933.00	0.0	$1 \rightarrow 0_1^+$			
3939.27	0.33(10)	78^{+46}_{-25}	3321.70	617.5	$1\text{–}3 \rightarrow 2_1^+$			
3952.26	0.391(34)	62(9)	3334.69	617.5	$1\text{–}3 \rightarrow 2_1^+$			
3963.79	0.44(18)	50^{+58}_{-25}	3963.71	0.0	$1,2 \rightarrow 0_1^+$			
3969.29	0.34(16)	76^{+94}_{-35}	3351.72	617.5	$\rightarrow 2_1^+$			
4033.89	0.31(12)	89^{+77}_{-35}	3416.31	617.5	$\rightarrow 2_1^+$			

[a]Values obtained from Ref. [35].
[b]Upper limits could not be determined due to uncertainty in the branching ratio. The branching intensity listed in Ref. [27] is incorrect due to improperly accounting for a background peak at this energy. The value listed in Ref. [27] should be used as an upper limit only.
[c]No branching intensity could be determined in Ref. [27].

of the final state depends on the details of the nuclear structure of the level, i.e., on the configuration of the wave function, whereas nonselective processes are those where the components of the wave function play no role in the population of the level, i.e., as observed in compound-nucleus reactions. Selective reactions by their very nature are critical for determining configuration assignments, and examples include one- and two-nucleon transfer reactions. Nonselective reactions, on the other hand, are crucial for building comprehensive level schemes and include fusion-evaporation reactions and the present $(n, n'\gamma)$ reaction.

In order to have a successful interpretation of the level scheme of ^{112}Cd, data from as many probes as possible will be considered, beginning with data from selective processes, and then consideration of the collective γ-ray decays. The goal is to attempt to identify the dominant configurations in levels up to the pairing gap (at approximately 2.5 MeV) and above, if possible. Figure 3 presents all levels in ^{112}Cd up to 3 MeV with configuration assignments suggested. As a basis for the interpretations, the language of the vibrational model is used in as much as it describes the nature of the levels. In some cases, the level is labeled by only one component of its wave function, which may not be the dominant one. Further, levels may be labeled with collective components even if they are not in agreement with detailed IBM-2 calculations as outlined in Sec. V, reflecting the limitation of the modeling.

A. Single-nucleon transfer data and two-quasiparticle states

One of the most powerful tools that can be used in nuclear spectroscopy is single-nucleon-transfer reactions. Single-nucleon transfer provides vital information concerning the microscopic nature of the levels. When starting with an odd-A target and studying transitions to an even-even system, the initial state is typically a one quasiparticle state, $|j_t\rangle$, with single-particle angular momentum $j_t = I_t$ the ground-state angular momentum, provided that deformation and mixing effects are small. Since the transfer operator is either a one-particle creation or annihilation operator, the final-state components sampled are two-quasiparticle configurations of the form $|j_t\rangle \otimes |j_{tr}\rangle$, with j_{tr} being the transferred angular momentum. Levels in ^{112}Cd have been studied [38,39] via the ^{111}Cd$(d, p)^{112}$Cd and ^{113}Cd$(\vec{d}, t)^{112}$Cd single-neutron transfer reactions. Shown in Fig. 4 are spectroscopic strengths from the ^{113}Cd$(\vec{d}, t)^{112}$Cd reaction obtained with polarized 20 MeV deuterons [38]. The ^{113}Cd target ground state has the configuration $0.77|s^\nu_{1/2}\rangle + 0.63[|2_1^+ \otimes d^\nu_{5/2}\rangle]^{1/2}$, where 2_1^+ refers to the first 2^+ state in ^{112}Cd [40]. Therefore, the final-state configurations that may be populated are of the form $[|s^\nu_{1/2}\rangle \otimes |j^\nu_{tr}\rangle]^{I_f}$ and $[[|2_1^+ \otimes d^\nu_{5/2}\rangle]^{1/2} \otimes |j^\nu_{tr}\rangle]^{I_f}$. From Fig. 4 one can immediately see that, below 2.5 MeV, the only strongly populated states are the ground state and the 617-keV 2^+ one-phonon level. One has to then look above ≈2.5 MeV,

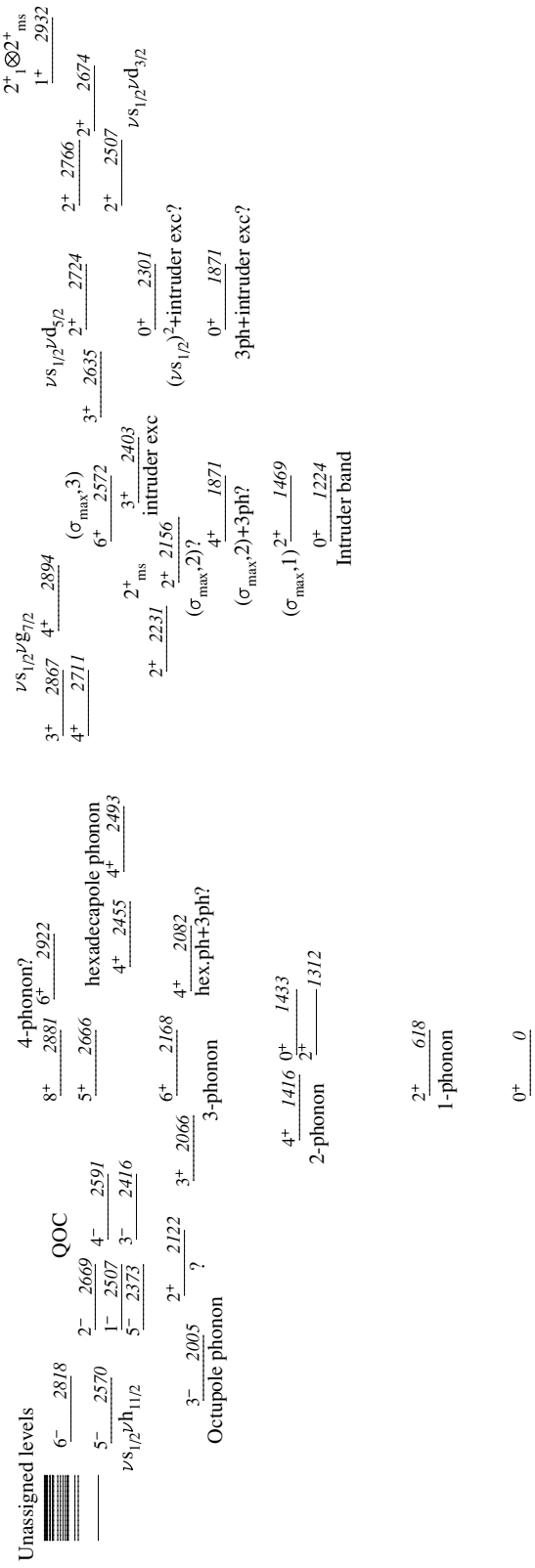

FIG. 3. Interpretation of levels in ^{112}Cd from all available data. Labels are suggested for the dominant configuration in the wave function with the assumption that ^{112}Cd is a vibrational nucleus. There is a breakdown in the assignment of levels above 1.6 MeV as multiphonon in nature, with very few levels in agreement with detailed calculations (see Sec. V).

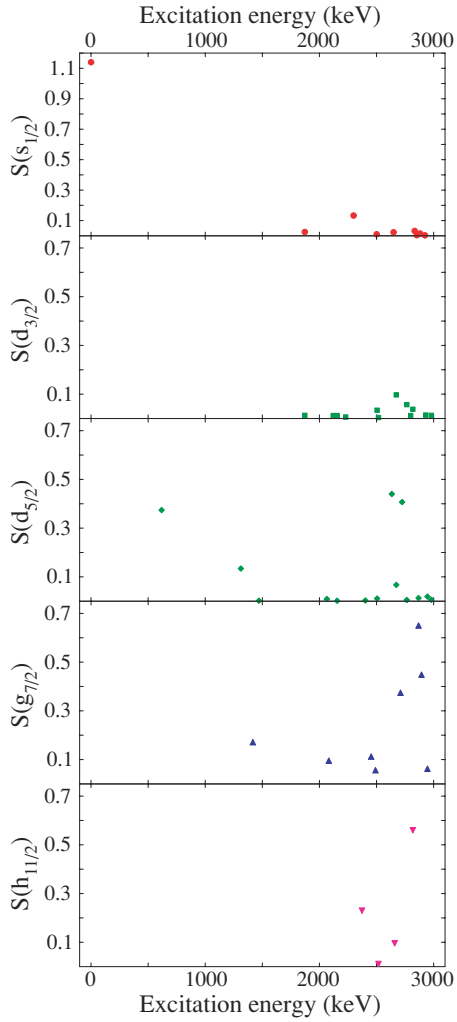

FIG. 4. (Color online) Results from the ^{113}Cd$(\vec{d},t)^{112}$Cd reaction obtained with polarized 20 MeV deuterons. Shown is a summary of the spectroscopic factors for each j transfer as a function of excitation energy. The data shown are from Ref. [38].

in the region where two-quasiparticle states begin to dominate over collective states (the pairing gap is ≈2.5 MeV) before observing other strongly-populated levels [38]. The two-phonon levels at 1312-keV and 1415-keV are only weakly populated. This indicates that, while in principle two-phonon levels could be populated via the $[|2_1^+\rangle \otimes d^\nu_{5/2}\rangle]^{1/2}$ component in the target-ground-state wave function, these transitions do not contribute strongly to the observed spectroscopic strengths. Strongly populated levels observed in the (d,t) or (d,p) reaction are therefore labeled as the $[|s^\nu_{1/2}\rangle \otimes |j^\nu_{tr}\rangle]^{I_f}$ configuration.

Since both the $d_{3/2}$ and $d_{5/2}$ neutron states lie relatively close to the Fermi surface, both are expected to contribute to the observed $l=2$ transitions in both the (d,p) and (d,t) reactions. The $(\vec{d},t)$ reaction study by Blasi *et al.* [38] could differentiate between $d_{3/2}$ and $d_{5/2}$ contributions through an analyzing power analysis, whereas the (d,p) study [39] could not. However, since the (d,p) reaction predominantly populates states located above the Fermi level whilst the (d,t)

reaction favors the population of states below the Fermi level, those states that are populated strongly with $l = 2$ transitions in the (d, p) reaction and weakly in the (d, t) reaction will be interpreted as involving $d^{\nu}_{3/2}$ transfer.

The coupling of the $s_{1/2}$ neutron with the expected low-lying neutron-hole states, $g_{7/2}$ and $d_{5/2}$, should give rise to $3^+, 4^+$ levels $(s^{\nu}_{1/2} \otimes g^{\nu}_{7/2})$ and $2^+, 3^+$ levels $(s^{\nu}_{1/2} \otimes d^{\nu}_{5/2})$ that are populated strongly in the $(\vec{d}, t)$ reaction. The $s^{\nu}_{1/2} \otimes g^{\nu}_{7/2}\ 3^+$ state is assigned at 2867 keV, with the $g^{\nu}_{7/2}$ transfer strength divided amongst the 4^+ levels at 2711 and 2894 keV [38]. The $d_{5/2}$ transfer strength is dominantly in the one-phonon 617-keV level, and the 3^+ and 2^+ levels at 2635 and 2724 keV, respectively [38]. These latter levels are therefore assigned as predominantly the $s^{\nu}_{1/2} \otimes d^{\nu}_{5/2}$ configuration. Interestingly, these levels also appear to be strongly populated in the (d, p) reaction [39], implying nearly equal U^2 and V^2 parameters. It would be clearly desirable to repeat the (d, p) study with better resolution and higher deuteron beam energy.

The coupling of the $s_{1/2}$ neutron with the expected low-lying neutron particle states, $s_{1/2}$, $h_{11/2}$ and $d_{3/2}$, should give rise to a 0^+ state $(s^{\nu}_{1/2} \otimes s^{\nu}_{1/2})$, 5^- and 6^- levels $(s^{\nu}_{1/2} \otimes h^{\nu}_{11/2})$, and $1^+, 2^+$ levels $(s^{\nu}_{1/2} \otimes d^{\nu}_{3/2})$ that are populated strongly in the (d, p) reaction. Much of the $s^{\nu}_{1/2} \otimes s^{\nu}_{1/2}$ strength is expected to be contained in the ground state, as observed [38,39]. The next most strongly populated 0^+ state is the level at 2301 keV, which in the (d, p) reaction is populated nearly as strongly as the ground state, but much more weakly populated than the ground state in the (d, t) reaction [38,39]. No $l = 5$ transitions were observed in the (d, p) study [39], presumably due to the low intrinsic cross section for the low deuteron beam energy of 7.7 MeV used in that work, but strong $l = 5$ transitions were observed in the $(\vec{d}, t)$ study [38] to a 5^- level at 2570 keV and a 6^- level at 2818 keV. These are therefore assigned as the $s^{\nu}_{1/2} \otimes h^{\nu}_{11/2}$ configuration. The (d, p) work [39] observed three similarly strong $l = 2$ transitions to the 2^+ levels at 2507, 2674, and 2766 keV, none of which were populated strongly in the $(\vec{d}, t)$ study [38], hence these are suggested to have significant fragments of the $s^{\nu}_{1/2} \otimes d^{\nu}_{3/2}$ configuration. The lowest-lying 1^+ level at 2932 keV was also populated strongly in the (d, p) reaction, suggesting a large amplitude of the $s^{\nu}_{1/2} \otimes d^{\nu}_{3/2}$ component in its wave function. Figure 5 summarizes the configuration assignments from the single-neutron transfer studies.

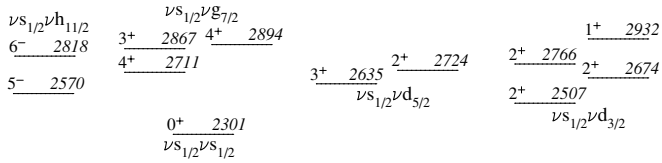

FIG. 5. Suggested two-quasiparticle configuration assignments based on the results of single-neutron-transfer reactions from Refs. [38,39]. In some cases, the transfer strength is fragmented over several levels.

B. Inelastic scattering reactions and one-phonon levels

The nucleus ^{112}Cd has been well studied using the inelastic scattering reactions (p, p'), $(\vec{d}, d')$, and (α, α'). Figure 6 displays results from a series of (p, p') and (d, d') studies [45–48], where the data are presented as reduced transition rates $B(X\lambda; I^{\pi}_f \rightarrow 0^+_{\text{g.s.}})$. These studies probe collective components in the final-state wave functions and are especially sensitive to one-phonon states since these have large transition matrix elements to the ground state. Thus, one-phonon states, such as the 617-keV one-phonon quadrupole state and the 2005-keV one-phonon octupole state are populated strongly. No other 2^+ or 3^- states are populated strongly in the reactions, consistent with very little fragmentation of the one-phonon quadrupole and octupole strength. On the other hand, there are three strong transitions $[B(E4) \approx 8$ W.u.$]$ to 4^+ levels between 2.0 and 2.6 MeV, and four other transitions with $B(E4)$ values larger than 1 W.u. to 4^+ states below 3 MeV are observed. These can be interpreted as the fragmentation of the one-phonon hexadecapole state, with a summed strength of 37 W.u. below 3 MeV, as shown in Fig. 3. The IBM1-*sdg* calculations of Hertenberger *et al.* [48] reproduced the strong fragmentation of the one-phonon hexadecapole strength.

The analysis of the data [48] revealed that the 2^+_1, 2^+_2, and 4^+_1 levels are nearly pure vibrational states, while the 2^+_3 level is a nearly pure intruder state. In contrast, the 0^+_2 and 0^+_3 wave functions each contain ≈50% of the two-phonon state. This selective mixing gives evidence of the presence of the $O(5)$ symmetry in the normal phonon and intruder states [13].

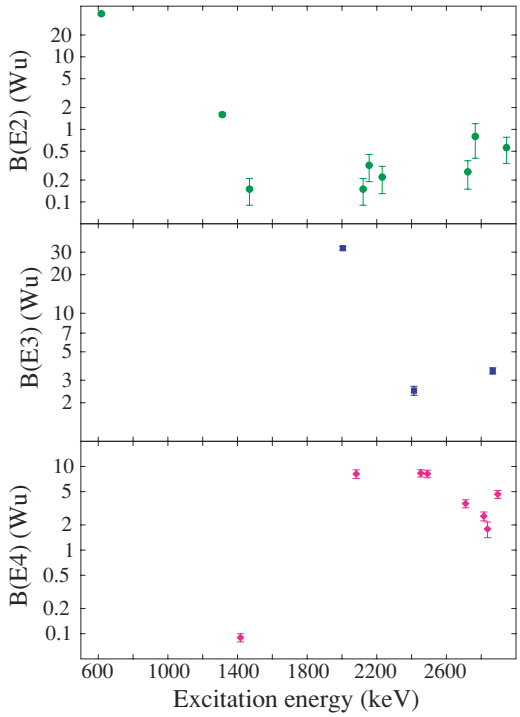

FIG. 6. (Color online) Results from the ^{112}Cd(p, p') and ^{112}Cd(d, d') reactions. For ease of comparison with electromagnetic transitions, the inelastic scattering transition matrix elements $B(E\lambda; J_f \rightarrow 0^+_{\text{g.s.}}) = |M(E\lambda \uparrow)|^2/(2j + 1)$ are expressed in W.u. The data shown are from Refs. [45–48].

C. Collective electromagnetic transitions and multiphonon levels

The use of nonselective reactions, like the ^{110}Pd$(\alpha, 2n\gamma)^{112}$Cd [41–43] and ^{112}Cd$(n, n'\gamma)$ [23,27–29] reactions, offer the advantage that levels are populated in a statistical manner, independent of their structure. The limitation for observation of individual levels in these types of experiments arises from angular momentum, detector sensitivity, and resolution considerations. The $(\alpha, 2n\gamma)$ reaction is limited, in this particular case, to approximately $I \leqslant 14$ and levels within ≈ 1.5 MeV of the yrast line [43]. The $(n, n'\gamma)$ reaction is limited to levels with $I \leqslant 6$, and while levels are populated up to very high excitation energy, the ability to detect them can be limited by the complexity of the spectra observed in the Ge detector [27]. The combination of data from both reactions, together with results from the selective reactions discussed above, has resulted in a comprehensive level scheme up to 3.4 MeV in excitation energy [27]. The $(n, n'\gamma)$ reaction offers the advantage that level lifetimes can be determined using DSAM where the level feeding can be controlled by the judicious choice of the bombarding neutron energy.

1. Multiphonon states

The one-phonon 2^+ level at 617.5 keV has a measured $B(E2; 2^+_{1ph} \rightarrow 0^+_{\text{g.s.}})$ value of 30.2 ± 0.3 W.u. [35] that sets the scale for quadrupole collectivity in ^{112}Cd. The two-phonon triplet of states, $0^+, 2^+$, and 4^+, have been assigned at 1433.3 keV, 1312.4 keV, and 1415.6 keV, respectively, on the basis of their energies and $E2$ transition strengths. While the 2^+ and 4^+ levels have enhanced transitions to the one phonon level of 15 ± 3 W.u. and 61 ± 6 W.u., respectively, the transition strength of the 0^+ member is thought to be reduced due to mixing with the intruder 0^+ band head. The $\rho^2(E0)$ strength has been measured for the $0^+_3 \rightarrow 0^+_1$ transition to be $(0.48 \pm 0.11) \times 10^{-3}$, and $\rho^2(E0; 0^+_3 \rightarrow 0^+_2) = (8.1 \pm 1.9) \times 10^{-3}$. $E0$ transitions are forbidden in the $U(5)$ limit of the IBM [50], and thus the small magnitude of the $\rho^2(E0; 0^+_3 \rightarrow 0^+_1)$ value agrees with this expectation. As mentioned previously, the analysis [48] of inelastic scattering data indicates strong mixing consistent with the $U(5) - O(6)$ model [14] expectations (see Fig. 4 in Ref. [23]).

The transitions from the three-phonon states were investigated in Ref. [23] where it was found that the spin 3^+ and 4^+ members of three-phonon quintuplet had decay patterns that matched well with expectations and calculations. Lifetimes for the suggested [14,17,23,43,44]0^+ and 6^+ members at 1871 keV and 2168 keV, respectively, could not be obtained due to unresolved transitions in both cases. The possible mixing of the 0^+_{3ph} level with an intruder excitation will be discussed below.

The spin 2^+ member, suggested [23,43,44] to be at 2121.6 keV, had serious discrepancies from expectations in that it had enhanced transition rates to the 0^+_2 and 0^+_3 levels only [23]. In an harmonic vibrator interpretation, the 2^+ three-phonon level should have a $B(E2; 2^+_{3ph} \rightarrow 0^+_{2ph})$ value of 42.8 W.u., and $B(E2; 2^+_{3ph} \rightarrow 2^+_{2ph})$ and $B(E2; 2^+_{3ph} \rightarrow 4^+_{2ph})$ values of 17.5 W.u. and 31.5 W.u., respectively. With the increased knowledge of decay of higher-excited 2^+ states now available, the "missing" 2^+ state $B(E2)$ strength can be sought. Extracted from Table II are the $B(E2; 2^+ \rightarrow I^+_f)$ values for decays from all the 2^+ states below 3 MeV into the assigned two-phonon levels, as well as the 0^+ and 2^+ members of the intruder band, and displayed in Fig. 7. The transitions are labeled by their $B(E2)$ values; dashed lines represent transitions where only upper limits could be determined. Since the two-phonon 0^+ state and 0^+ intruder band head are strongly mixed according to IBM calculations, the sum of the strength into both levels can be compared to the expectations. The observed $\Sigma B(E2; 2^+ \rightarrow 0^+_2, 0^+_3)$ value is 81 ± 17 W.u., including the $2^+_I \rightarrow 0^+_2$ transition, or 35 ± 9 W.u. excluding the $2^+_I \rightarrow 0^+_2$ transition. This latter amount is in reasonable agreement with the harmonic oscillator value. The observed strength into the 2^+ two-phonon level (the nearby intruder 2^+ is not included since the mixing should be minimal in this case according to the IBM [13,14,17,23]) is only $6.2^{+6.7}_{-0.7}$ W.u., far less than the 17.5 W.u. for the harmonic oscillator. No strength is observed into the 4^+ level of the two-phonon triplet. The latter is particularly interesting since it is not due to a lack of experimental sensitivity – transitions to the 2^+ states at 1312 keV and 1469 keV are clearly observed – rather, it is the apparent lack of even weakly-collective transitions from 2^+ levels into the 4^+ two-phonon level.

As shown in Fig. 3, possible candidates for four-phonon levels include the 2666-keV 5^+, 2881-keV 8^+, and 2922-keV 6^+ levels. Unfortunately, lifetimes are not available for these levels and thus their absolute transition rates are unknown. No other four-phonon candidates could be identified.

2. Intruder states

It is well established [6–8] in nuclei near $Z = 50$ that the promotion of a pair of particles below the $Z = 50$ shell into levels above the shell gap results in an excitation with a degree of deformation greater than that possessed by the ground state due to the increase in the number of p-n interactions. These excitations, labeled as intruder states, have energies relative to the ground state that vary as a function of the valence neutron number and approach a minimum near midshell. In the Cd isotopes, the midshell nucleus is $^{114}_{48}$Cd$_{66}$ and thus the intruding proton $2p4h$ configuration 0^+_I will be near a minimum in excitation energy in ^{112}Cd. The intruder band, which is a manifestation of a pairing excitation, has an enhanced two-proton-transfer cross section for population of the 0^+ band head [49], consistent with this interpretation. The low-lying members of the intruder band have been well-documented in many publications, and are delineated in ^{112}Cd in the $(\alpha, 2n)$ reaction work [41–43], where it was observed up to spin 8^+.

The intruder band has been described [12,14,17,23,43] in the $O(6)$ limit with two additional proton bosons. The "ground state" of the intruder configuration is shifted upward in energy relative to the normal ground state by the amount $\Delta + \langle Q \cdot Q \rangle$ where Δ is the pairing energy correction and $\langle Q \cdot Q \rangle$ is the relative energy gained due to the quadrupole proton-neutron interactions [12,17]. The $O(6)$ limit is chosen

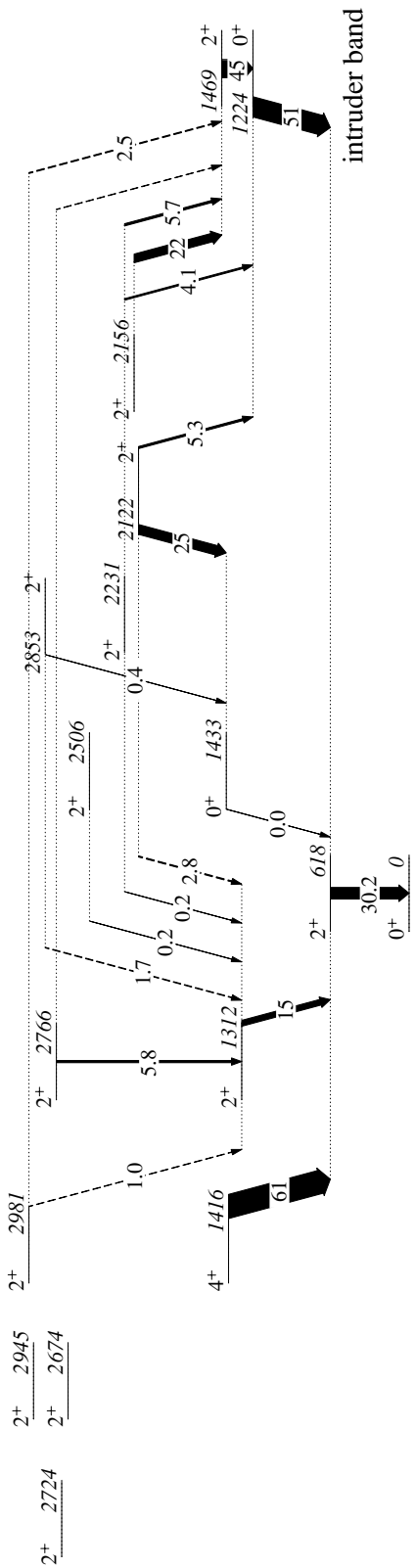

FIG. 7. Partial experimental level scheme showing the $B(E2; 2^+ \rightarrow I_f^+)$ values for decay into the assigned two-phonon and $0^+, 2^+$ members of the intruder band for all 2^+ states below 3 MeV excitation energy. The transitions are labeled with their $B(E2)$ values in W.u., and dashed lines indicate transitions where upper limits could be determined.

because the energy ratio E_{4^+}/E_{2^+} for the intruder band is $\approx$2.6, very close to the value expected (of 2.5) for a γ-soft vibrator. The degree of deformation is greater than that of the ground state, as evidenced by a moderately strong $E0$ transition between the intruder band head and the ground state of $\rho^2(E0) = (37 \pm 11) \times 10^{-3}$, and between the 2_I^+ and 2_1^+ levels of $\rho^2(E0) = (31 \pm 20) \times 10^{-3}$ [50]. Using the $O(6)$ limit, an intruder excitation spectrum as shown in Fig. 8 is expected. As will be seen below, IBM-2 calculations taking into account mixing between the normal phonon and intruder states perturb the decay patterns somewhat, but many features in Fig. 8 will still be recognizable.

It is clear from examining Fig. 8 that, apart from the energies of the low-lying members of the intruder yrast band, the intruder configuration is not well represented by the pure $O(6)$ limit of the IBM. Deviations appear immediately when examining the nonyrast intruder states. However, it should be noted that in Fig. 8 the theoretical values assume a pure $O(6)$ structure without mixing with the normal phonon or quasiparticle states. It is known that such mixings occur that perturb both the level energies and decay transition rates (see, e.g., Refs. [13,14]), as will be outlined in Sec. V. The lowest energy 2^+ state that could possibly be assigned as the $(\sigma_{max}, \tau = 2)$ state is the level at 2156 keV, nearly 300 keV above the 1871-keV 4^+ level. The $B(E2; 2156 \rightarrow 2_I^+)$ value is $\approx$1/3 of its expected value of 62 W.u.; in fact, the sum of the $B(E2; 2^+ \rightarrow 2_I^+)$ strength for all 2^+ levels below 3 MeV is <30 W.u. Unfortunately, the lifetimes of the higher-spin members of the intruder yrast band could not be determined in the present $(n, n'\gamma)$ study. The only other reasonable candidates for nonyrast (σ_{max}, τ) states are the 3^+ level at 2403 keV and the 0^+ levels at 1871 keV and 2301 keV. The 2403-keV level has $B(E2)$ values that do not match the expected $O(6)$ selection rules, however. While there is an enhanced $B(E2; 3^+ \rightarrow 4_I^+)$ value, there is a large $B(E2; 3^+ \rightarrow 2_I^+)$ value of 21 W.u. for this forbidden transition. Even the assigned 4^+ member of the intruder yrast band may have serious departures from an intruder character in its decay. The branching ratios for the decay of the 1871-keV 4^+ level could not be determined in the present study, due to the proximity of the 1871-keV 0^+ level. However, the assumption can be made that the intensities of the decaying γ rays in the $(\alpha, 2n)$ study by Délèze *et al.* [43] are unlikely to be perturbed by decays from the 0^+ level as it would be extremely weakly populated in the reaction. Therefore, the branching intensities for the $4_I^+ \rightarrow 2_I^+, 4_I^+ \rightarrow 4_1^+, 4_I^+ \rightarrow 2_2^+$, and $4_I^+ \rightarrow 2_1^+$ are 0.163 ± 0.001, 0.087 ± 0.001, 0.502 ± 0.002, and 0.249 ± 0.002, respectively. Using these values, "relative $B(E2)$'s" for the respective decays are 100, 25.1 ± 0.4, 59.5 ± 0.5, and 0.52 ± 0.01. While it is gratifying that the $4_I^+ \rightarrow 2_I^+$ transition dominates, the large value for the $4_I^+ \rightarrow 2_{2ph}^+$ transition of $\approx$60% of the $B(E2; 4_I^+ \rightarrow 2_I^+)$ value implies that a significant degree of mixing must occur.

Using a similar argument needed for the 1871-keV 4^+ level, it is possible to extract the relative $B(E2)$ values from the data for the 0^+ level at 1871 keV. In the $(n_{\rm th}, \gamma)$ reaction on ^{111}Cd, with a ground state spin of $\frac{1}{2}^+$, the spin 4^+ level at 1871 keV should not be populated to an appreciable extent. The intensities of the 402-keV, 558-keV and 1253-keV

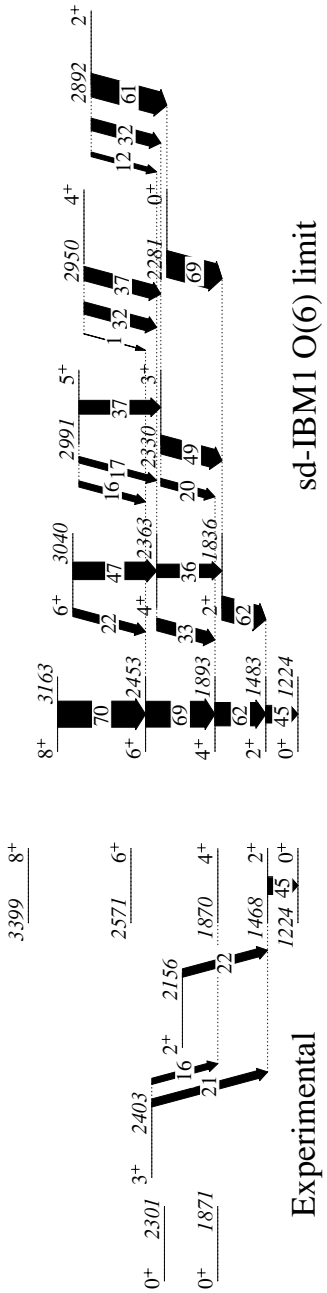

FIG. 8. Partial level scheme showing the $B(E2; I_i^+ \rightarrow I_f^+)$ values for decay into the intruder levels. On the right are shown the expected values based on the $O(6)$ limit of the IBM-1, normalized to the experimental $2_I^+ \rightarrow 0_I^+$ value of 45 W.u. and the observed excitation energy of 1224 keV.

γ rays from that reaction [44] can therefore be used to determine the branching ratios for decays from the 1871-keV 0^+ level. Adopting these intensities, branching intensities for the $0^+ \rightarrow 2_3^+$, $0^+ \rightarrow 2_2^+$, and $0^+ \rightarrow 2_1^+$ transitions are determined to be 0.190 ± 0.029, 0.338 ± 0.020, and 0.472 ± 0.025, respectively. These yield "relative $B(E2)$" values of 290 ± 47, 100, and 2.5 ± 0.2 for the respective transitions. If these data are correct, it implies that the suggested 0^+ member of the three-phonon quintuplet has a very perturbed decay pattern in that the strongest $B(E2)$ value is for the decay into the 2^+ member of the intruder band. In fact, from these considerations, one might be tempted to assign the 1871-keV 0^+ level as an excitation based on the intruder configuration, and there may be strong mixing between the 0_{3ph}^+ and intruder excitations as expected in the $U(5) - O(6)$ model [14] (see Fig. 4 in Ref. [23]). This intruder excitation cannot be identified as the $(\sigma_{max}, \tau = 3)$ level as expected from the $O(6)$ representation, however, since this level should have an enhanced decay into the $(\sigma_{max}, \tau = 2)$ 2^+ state. The 0^+ level at 2301 keV, which has a significant $(\nu s_{1/2})^2$ component, has a $B(E2; 0^+ \rightarrow 2_I^+)/B(E2; 0^+ \rightarrow 2_1^+)$ ratio of $\approx$16; unfortunately, a lifetime measurement for this level was not possible. It may, however, represent another fragment of the excited intruder configuration that is present in the 1871-keV level.

The conclusion to be reached at this point is that, while the higher-spin members of the three-phonon multiplet continue to display not only a collective character, but also the degree of $E2$ collectivity expected, the lower-spin members encounter serious deficiencies with the expectations of the harmonic oscillator. As will be discussed below, full calculations taking into account the mixing between the normal phonon and intruder states can only partially explain the discrepancies.

D. Proton and neutron content

The well-known relation [51] for the quadrupole deformation parameters $\beta^{(2)}$ observed in inelastic scattering is

$$\beta_{pp'} = \frac{N V_{pn} \beta_n + Z V_{pp} \beta_p}{N V_{pn} + Z V_{pp}}, \tag{4}$$

where $\beta_{pp'}$ is the deformation parameter observed in (p, p') scattering and V_{pn} and V_{pp} are nucleon-nucleon interaction potentials. Together with the relation $\beta_{EM} = \beta_p$ (where only electric transitions are considered) and with the approximation [51] that the interaction potentials satisfy $V_{pn} \approx 3V_{pp}$, the expression

$$\beta_n = \left(1 + \frac{Z}{3N}\right) \beta_{pp'} - \frac{Z}{3N} \beta_p \tag{5}$$

is obtained. The isoscalar deformation parameter is defined as

$$\beta_0 = \frac{N\beta_n + Z\beta_p}{A} \tag{6}$$

and the isovector deformation parameter, which contains important structure information as it reflects the difference between neutron and proton contributions to the collective excitations, is

$$\beta_1 = \frac{N\beta_n - Z\beta_p}{N - Z}. \tag{7}$$

Thus, if the transition rates are known from (p, p') inelastic scattering and from a purely electromagnetic process, the isoscalar and isovector deformation parameters can be determined. Since ^{112}Cd has 64 neutrons and 48 protons, one would expect that most levels would have a greater neutron than proton contribution, i.e., $N\beta_n > Z\beta_p$ [which also leads to $B(E2 : pp') > B(E2 : \mathrm{EM})$], or a *positive* isovector

deformation parameter β_1. While strictly valid only for one-step reactions to collective states, this kind of analysis can be extended to higher excited states provided that indirect excitations in the (p, p') data are considered. Using the values of $\beta_{pp'}$ from de Leo *et al.* [45] (the first-order transition deformation parameter is used) the isoscalar and isovector deformation parameters are extracted as shown in Fig. 9. As can be seen, the isovector parameters are positive, except for the case of the 2_3 level, the intruder state at 1469 keV. The negative value for the isovector β_1 implies a greater role for the protons in that excitation, as expected.

V. IBM-2 CALCULATIONS

The results of the present work are compared with IBM-2 calculations similar to those in the work of Délèze *et al.* [42]. The computer codes NPBOS and NPEM [52] were modified to enlarge the number of states calculated so that the experimental results could be compared to detailed calculations to higher excitation energy. The normal states and intruder states were calculated separately using the Hamiltonian

$$\hat{H} = \epsilon(d_\pi^\dagger \tilde{d}_\pi + d_\nu^\dagger \tilde{d}_\nu) + \hat{V}_{\pi\pi} + \hat{V}_{\nu\nu} + \kappa \hat{Q}_\pi \hat{Q}_\nu + \hat{M}_{\pi\nu}, \quad (8)$$

where

$$\hat{V}_{\rho\rho} = \sum_{L=0,2,4} \frac{1}{2} C_{L_\rho} \sqrt{2L+1} [(d_\rho^\dagger d_\rho^\dagger)^{(L)} (\tilde{d}_\rho \tilde{d}_\rho)^{(L)}]^{(0)} \quad (9)$$

is the interaction between like bosons,

$$\hat{Q}_\rho = (s_\rho^\dagger \tilde{d}_\rho + d_\rho^\dagger s_\rho)^{(2)} + \chi_\rho (d_\rho^\dagger \tilde{d}_\rho)^{(2)} \quad (10)$$

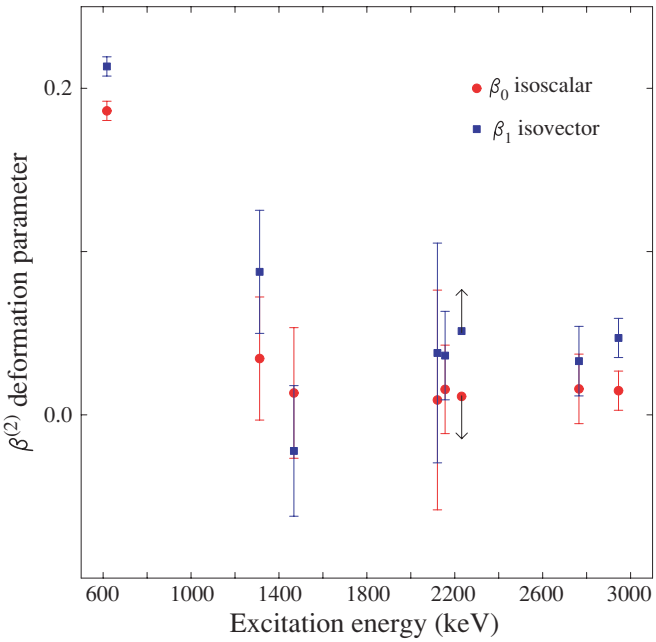

FIG. 9. (Color online) Extraction of the isoscalar (circles) and isovector (squares) deformation parameters for 2^+ states in ^{112}Cd. The data are extracted from the (p, p') deformation parameters given in Ref. [45] and from the electromagnetic transition rates (see text for details).

represents the quadrupole-quadrupole interaction between proton and neutron bosons, and

$$\hat{M}_{\pi\nu} = -\sum_{k=1,3} 2\xi_k (d_\pi^\dagger d_\nu^\dagger)^{(k)} (\tilde{d}_\pi \tilde{d}_\nu)^{(k)} + \xi_2 (d_\pi^\dagger s_\nu^\dagger - s_\pi^\dagger d_\nu^\dagger)^{(2)} (\tilde{d}_\pi s_\nu - s_\pi \tilde{d}_\nu)^{(2)} \quad (11)$$

is the Majorana interaction that acts on states that are not fully symmetric under the interchange of the proton and neutron degrees of freedom. The two separate configurations were then allowed to mix using the interaction

$$\hat{H}_{mix} = \alpha (s_\pi^\dagger s_\pi^\dagger + s_\pi s_\pi)^{(0)} + \beta (d_\pi^\dagger d_\pi^\dagger + \tilde{d}_\pi \tilde{d}_\pi)^{(0)}. \quad (12)$$

An energy gap, Δ, is added to the intruder configuration to shift its energy relative to the normal ground state before diagonalization takes place. With the wave functions determined, the electromagnetic transition rates are calculated via

$$\hat{T}(E0) = e_n^{(0)} (e_{\pi_n}^{(0)} d_{\pi_n}^\dagger \tilde{d}_{\pi_n} + e_{\nu_n}^{(0)} d_{\nu_n}^\dagger \tilde{d}_{\nu_n})^{(0)} + e_i^{(0)} (e_{\pi_I}^{(0)} d_{\pi_I}^\dagger \tilde{d}_{\pi_I} + e_{\nu_I}^{(0)} d_{\nu_I}^\dagger \tilde{d}_{\nu_I})^{(0)} \quad (13)$$

for $E0$ transitions,

$$\hat{T}(M1) = \sqrt{\frac{30}{4\pi}} \left(g_n (g_{\pi_n} d_{\pi_n}^\dagger \tilde{d}_{\pi_n} + g_{\nu_n} d_{\nu_n}^\dagger \tilde{d}_{\nu_n})^{(1)} + g_i (g_{\pi_I}^{(0)} d_{\pi_I}^\dagger \tilde{d}_{\pi_I} + g_{\nu_I} d_{\nu_I}^\dagger \tilde{d}_{\nu_I})^{(1)} \right) \quad (14)$$

for $M1$ transitions, and

$$\hat{T}(E2) = e_n^{(2)} (e_{\pi_n}^{(2)} \hat{Q}_\pi + e_{\nu_n}^{(2)} \hat{Q}_\nu) + e_I^{(2)} (e_{\pi_I}^{(2)} \hat{Q}_\pi + e_{\nu_I}^{(2)} \hat{Q}_\nu) \quad (15)$$

TABLE III. Values of parameters used in the Hamiltonian and for the computation of the transition rates. The values listed are taken from Ref. [42]. Minor adjustments of the effective $E2$ boson charges (in eb) and the effective boson g factors (in μ_N) have been made in order to reproduce the $B(E2; 2_1^+ \to 0_{gs}^+)$ and $B(M1; 1_1^+ \to 0_{gs}^+)$ values. All values are in MeV except χ which is dimensionless. The $E0$ effective charges are in $e\,fm^2$.

Normal configuration		Intruder configuration		Mixing parameters	
Parameter	Value	Parameter	Value	Parameter	Value
ϵ_d	0.88	ϵ_d	0.50	α	0.16
κ	−0.15	κ	−0.18	β	0.08
χ_ν	−0.10	χ_ν	−0.10	Δ	4.0
χ_π	−0.90	χ_π	0.40	$e_I^{(2)}/e_n^{(2)}$	1.35
$C_{0\nu}$	−0.25	$C_{0\nu}$	−0.25	g_I/g_n	1
$C_{2\nu}$	−0.12	$C_{2\nu}$	−0.12	$e_I^{(0)}/e_n^{(0)}$	1
$C_{4\nu}$	0.0	$C_{4\nu}$	0.04		
ξ_1	0.24	ξ_1	0.24		
ξ_2	0.04	ξ_2	0.04		
ξ_3	0.24	ξ_3	0.24		
$e_{\nu_n}^{(2)}$	0.0793	$e_{\nu_I}^{(2)}$	0.0793		
$e_{\pi_n}^{(2)}$	0.1360	$e_{\pi_I}^{(2)}$	0.1360		
g_{ν_n}	−0.0836	g_{ν_I}	−0.0836		
g_{π_n}	1.0868	g_{π_I}	1.0868		
$e_{\nu_n}^{(0)}$	0.25	$e_{\nu_I}^{(0)}$	0.25		
$e_{\pi_n}^{(0)}$	0.10	$e_{\pi_I}^{(0)}$	0.10		

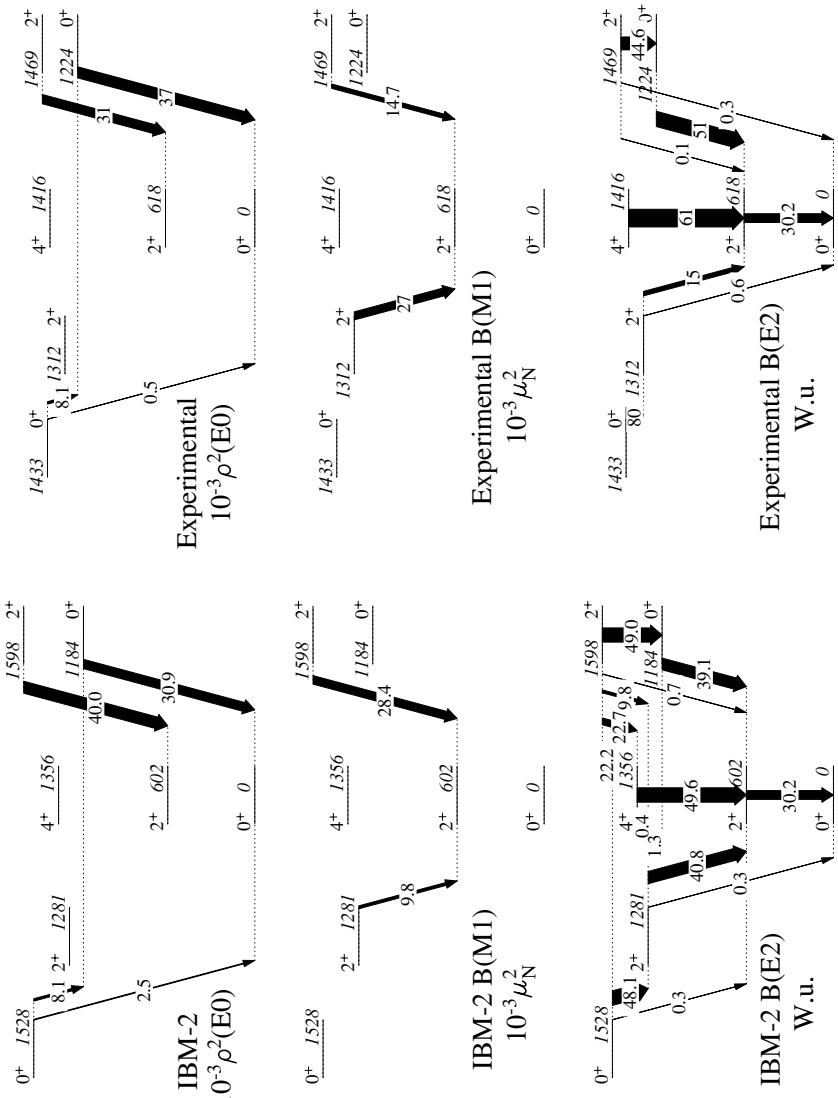

FIG. 10. Results of IBM-2 calculations (described in the text) for levels below 1.6 MeV in ^{112}Cd compared with experimental results (right). The top panel displays the $E0$ transitions labeled by their $10^{-3}\rho^2(E0)$ values, in the middle panel the transitions are labeled by their $B(M1)$ values in units of $10^{-3}\mu_N^2$, and in the bottom by their $B(E2)$ values, where greater than 0.1 W.u.

for $E2$ transitions where the operator $\hat{Q}$ is defined in Eq. (10). For the calculations, the same value for the χ parameters are used in the Hamiltonian as for the electromagnetic transition rates (the consistent Q formalism). The parameters used, taken from Ref. [42] where they were determined both phenomenologically and also using an OAI mapping procedure [53,54], are listed in Table III.

The effective charges used in the calculation of the transition rates are determined by normalizing to selected transitions in ^{112}Cd ($M1$, $E2$) or by adopting previously used values ($E0$). Minor adjustments of the $E2$ effective charges and boson g factors from the work by Délèze *et al.* [42] were made so that the experimental $B(E2; 2_1^+ \rightarrow 0^+_{\text{g.s.}})$ and $B(M1; 1_1^+ \rightarrow 0^+_{\text{g.s.}})$ values were reproduced. The $E0$ effective charges were taken from the work of Giannatiempo *et al.* [55] where fits were performed to the ^{110,112,114}Cd isotopes. The results of the calculations for the states below 1.5 MeV, i.e., the two-phonon states and the first two members of the intruder band, are shown in Fig. 10 compared with the experimental values. As can be seen, there is very good agreement with the $E0$ rates. For the $E2$ transitions, the $B(E2; 2_2^+ \rightarrow 2_1^+)$ value is observed to be much less, (15 ± 3 W.u.) than predicted, (41 W.u.) while the $B(E2; 0_3^+ \rightarrow 2_2^+)$ value is observed to be much larger (80 ± 12 W.u.) than predicted (48 W.u.). The calculated $B(M1; 2_3^+ \rightarrow 2_1^+)$ value is nearly a factor of 3 larger than the $B(M1; 2_2^+ \rightarrow 2_1^+)$ value, whereas experimentally the reverse is true. Thus, already at the two-phonon level, discrepancies between experiment and calculation emerge. The vanishing of the $0_3^+ \rightarrow 2_1^+$ transition can only be reproduced by a destructive interference between the two-phonon and intruder transition amplitudes; even a slight change in the parameters results in a collective $0_3^+ \rightarrow 2_1^+$ transition contrary to experiment. A similar vanishing of the $0_3^+ \rightarrow 2_1^+$ transition in other Cd isotopes (see, e.g., Ref. [56]) remains one of the outstanding problems with the phonon-intruder picture.

The results of the calculation for all levels below 3 MeV are given in Figs. 11 and 12, where the arrows are labeled by the $B(E2)$ values in W.u. for the transition (only those $\geqslant$ 5.0 W.u. are shown). As expected, collective transitions persist up to high energies. Although mixing causes the strength to

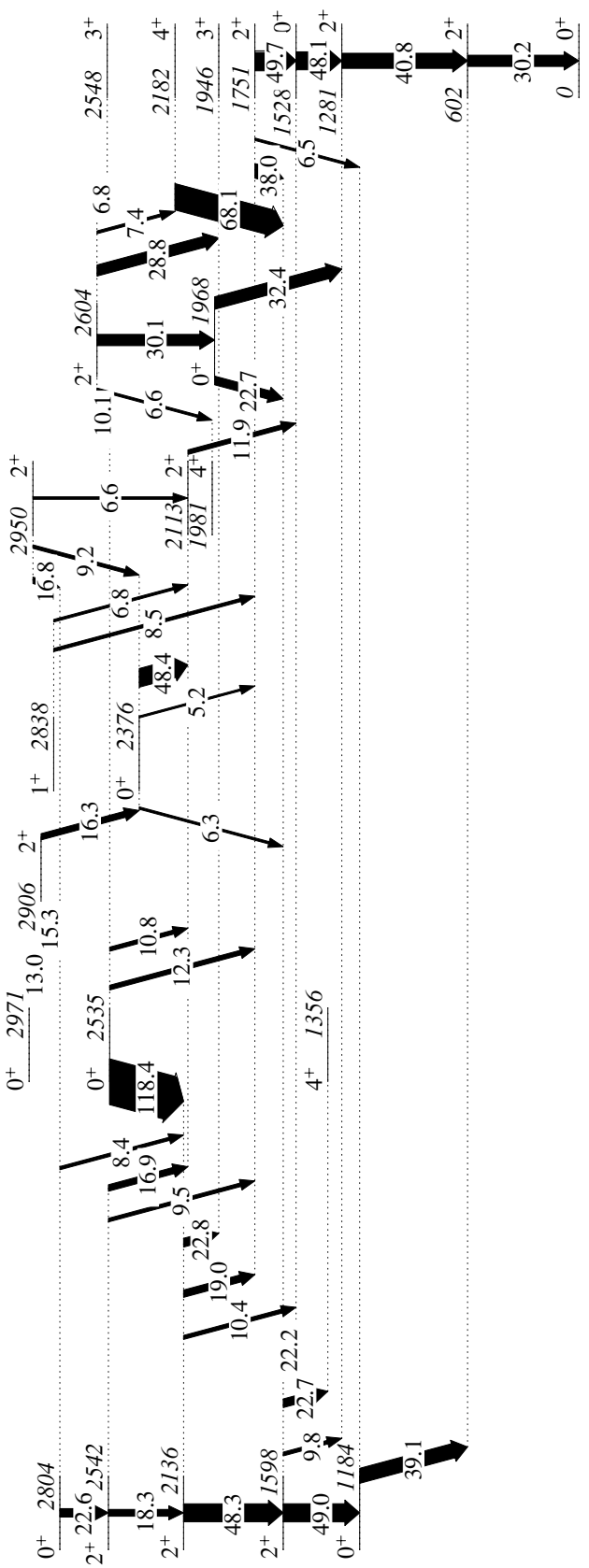

FIG. 11. Results of IBM-2 calculations (described in the text) for states with spins 0^+ to 2^+ in ^{112}Cd. Only transitions with $B(E2)$ values greater than 5 W.u. are shown.

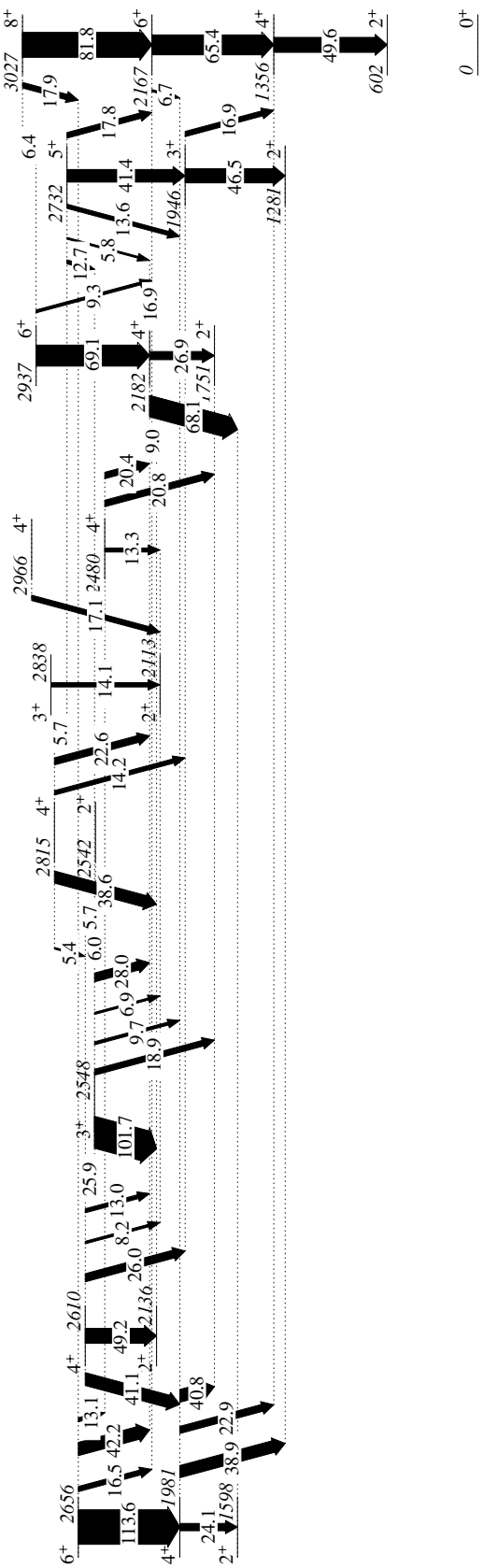

FIG. 12. Results of IBM-2 calculations (described in the text) for states with spins 3^+ to 8^+ in ^{112}Cd. Only transitions with $B(E2)$ values greater than 5 W.u. are shown.

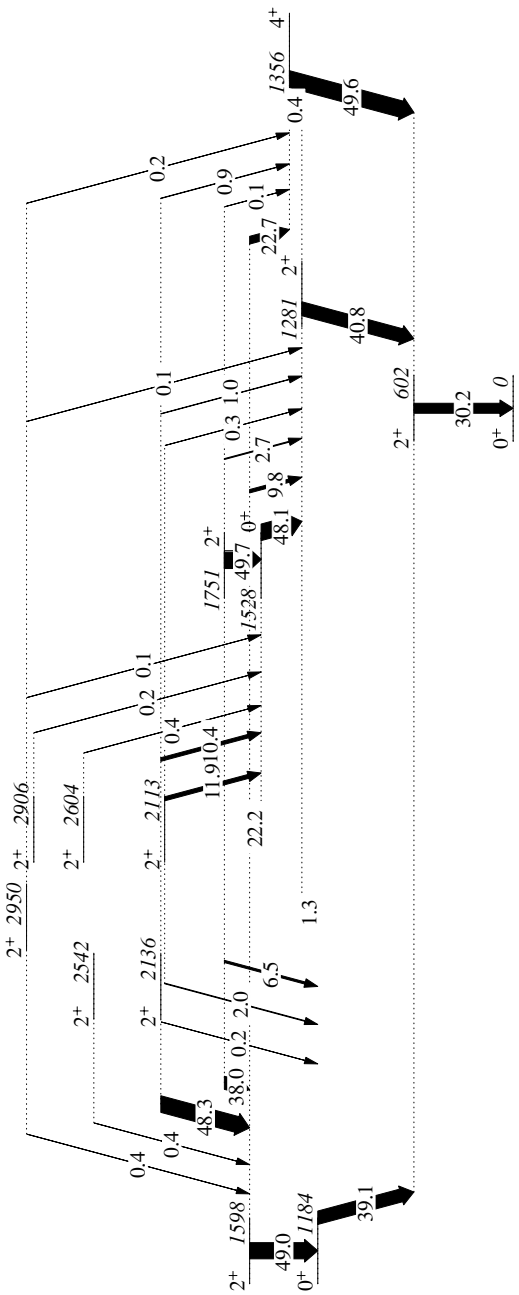

FIG. 13. Results of IBM-2 calculations (described in the text) for 2^+ states below 3 MeV in ^{112}Cd. Only transitions with $B(E2)$ values greater than 0.1 W.u. into the 0^+ and 2^+ members of the intruder band and the two-phonon triplet are shown.

be shared amongst many levels, it is not diminished by a substantial amount. Figure 13 displays in detail the predicted decay of the 2^+ states into the 0^+ and 2^+ members of the intruder band, and into members of two-phonon triplet. The total calculated $E2$ strengths for decays from 2^+ levels into the 2^+ and 4^+ two-phonon states, excluding decays that experimentally correspond to transition energies less than 100 keV, i.e., the $0_3^+ \rightarrow 2_2^+$ and $2_I^+ \rightarrow 4_1^+$ decays, are 13.9 W.u. and 1.2 W.u., in reasonable agreement with the experimental values of $6.2^{+6.7}_{-0.7}$ W.u. and no strength observed, respectively. While the IBM-2 calculations yield a similar number for the $\Sigma B(E2; 2^+ \rightarrow 2^+_{2ph})$ value as obtained in the harmonic oscillator limit, the $\Sigma B(E2; 2^+ \rightarrow 4^+_{2ph})$ value is more than an order of magnitude smaller than the harmonic oscillator. This arises because in the IBM-2 calculation the first 2^+ intruder state strongly mixes with the three-phonon 2^+ state such that a constructive interference occurs for the matrix elements for the (unobserved) $2_3^+ \rightarrow 4_1^+$ decay, whilst destructive interference occurs, resulting in a nearly complete cancellation of the matrix elements, for the $2_4^+ \rightarrow 4_1^+$ decay. For the calculated decays into the 0_2^+ and 0_3^+ states, using the same restriction as above, the summed $B(E2)$ values amount to 57.7 W.u. and 13.9 W.u. giving a total of 71.6 W.u., in good agreement with the observed amount of 81 ± 17 W.u. Since the calculated and observed $B(E2)$ value for the $2_3^+ \rightarrow 0_2^+$ transition are in excellent agreement, the conclusions are not altered significantly by removing this transition from the sum. Thus, the *summed* $E2$ strength for decays into the low-lying $0^+, 2^+$, and 4^+ states are reproduced well by the IBM-2 calculations.

Having found that the summed strength into the low-lying states compares favorably, attention can be focused on the states at higher excitation energy and their individual decays. From Figs. 11 and 12, it is apparent that there are predicted to be a large number of very collective transitions occurring at high excitation energy. Experimentally, it becomes more difficult to observe these types of transitions due to the increased competition with noncollective, high-energy branches. A much more restricted view is therefore taken in comparing the calculated and observed $B(E2)$ values. Shown in Fig. 14 are the calculated (left) and experimental (right) levels with *selected* $E2$ decay branches. Experimentally, the selection criteria are that the levels have, or that may be reasonably *expected* to have, collective γ decays above several W.u. For the calculated level scheme, an approximate correspondence is attempted to match the experimental levels, and the low-energy transitions, likely to be below the observational threshold, are removed.

In the excitation energy region expected for the three-phonon states, near 2 MeV, a candidate 0^+ member is the level observed at 1871 keV. Assuming that the above determined branching ratios are correct, the 1871-keV 0^+ level has a relative $B(E2; 0^+ \rightarrow 2_I^+)$ value that is nearly a factor of 3 larger than the $B(E2; 0^+ \rightarrow 2^+_{2ph})$ value, effectively ruling out its identification as the 0^+ three-phonon level that is calculated to have a $B(E2; 0^+ \rightarrow 2^+_{2ph})$ approximately 50% *larger* than the $B(E2; 0^+ \rightarrow 2_I^+)$ value. The 4^+ level observed at 1871 keV, also for which the branching ratios were suggested above, has its favored decay to the 2_I^+ level indicative of an intruder character. The calculated decay pattern for the 4_2^+ level, however, has more enhanced decays into the 2^+ and 4^+ two-phonon states, despite the fact that its wave function is slightly more than 50% intruder in origin. The calculated 4_3^+ level, on the other hand, decays nearly exclusively into the 2_I^+ level, despite the nearly 50% three-phonon content in its wave function. The strong mixing between the 4^+_{3ph} "normal" state

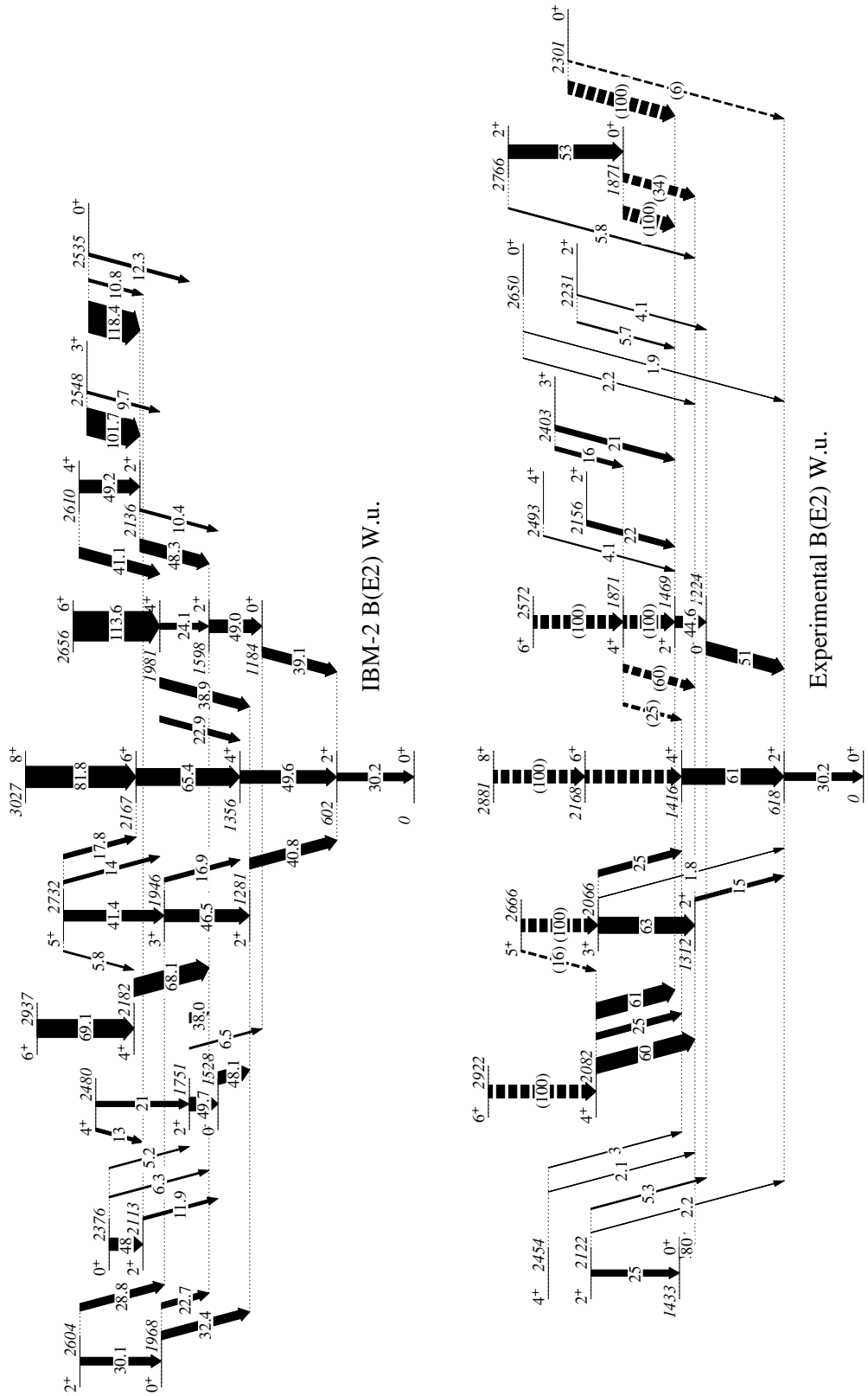

FIG. 14. Results of IBM-2 calculations (top) for selected levels and transitions that approximately match the observed collective levels (bottom). Dashed lines indicate relative $B(E2)$ values.

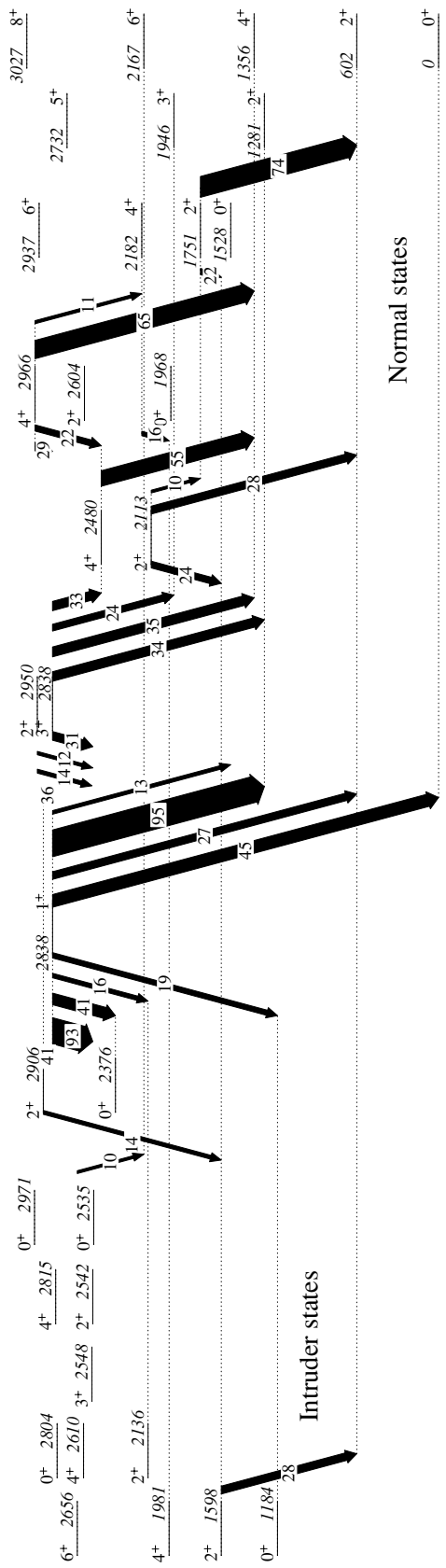

FIG. 15. Results of IBM-2 calculations (described in the text) for states in ^{112}Cd. Only transitions with $B(M1)$ values greater than 0.01 μ_N^2 are shown and are labeled in units of $10^{-3}\mu_N^2$.

and 4_I^+ intruder state, combined with the mixing between the 2_{3ph}^+ level and 2_I^+ intruder state, strongly perturbs the decay patterns in a nonintuitive way. Constructive interference occurs in the transition matrix elements for decay from the 4_2^+ level, whereas for the 4_3^+ level destructive interference occurs. In fact, the calculated decay pattern of the 4_2^+ state lead to its *assignment* [23] to the experimental 4_3^+ level that decays with 60 W.u. to both the 2_{2ph}^+ and 2_I^+ levels and 25 W.u. into the 4_{2ph}^+ state. However, reversing the order of the levels in such a way is not realistic since the perturbed decay pattern arises because of the details of the mixings; as in a two-level-mixing the higher-excitation energy state has destructive interference, whereas the lower-energy state undergoes constructive interference. (This situation is analogous to that of the 0^+ levels in ^{116}Cd [56].) Thus, in contrast to earlier conclusions concerning the nature of the three-phonon levels [23], the more extensive data now available implies that the description of the 4_2^+ and 4_3^+ levels is, in fact, unsatisfactory, and cannot be reproduced by the current model calculations.

As discussed above, none of the observed 2^+ levels near 2 MeV have decay patterns matching that expected for the 2^+ member of the three-phonon multiplet. The results of the calculations, as displayed in Fig. 14, are not in good agreement with the experimental results displayed in Fig. 7. The 2_4^+ level is predicted nearly 360 keV too low, and is calculated to have an enhanced decay into the 0_2^+ state and the 2_I^+ intruder level. No experimental level matches this decay pattern. The calculated 2_5^+ and 2_6^+ states are predicted to have enhanced decays to the 0_3^+, and 0_3^+ and 2_3^+ levels, respectively, of 12 W.u., and 10 and 48 W.u., respectively. These decay patterns approximately match those of the experimentally observed [28] 2_4^+ and 2_5^+ levels. The wave functions of these latter levels are not, however, dominated by three-phonon components. As outlined above, there are no suitable candidates for the 2^+ three-phonon member. In fact, of the three-phonon candidates [23], only the 3_1^+ level at 2065 keV (no lifetime is available for the 6_1^+ level) is in good agreement with the calculations.

Candidates for higher-phonon "normal" vibrational members, the 5^+ state at 2666 keV, the 6^+ level at 2922 keV, and the 8^+ level at 2881 keV, have no lifetime information available, and thus is it impossible to assess their collectivity. In fact, the only measurable collective decay is the $2^+(2766\text{ keV}) \rightarrow 0^+(1871\text{ keV})$ transition of 53 ± 9 W.u. This enhanced decay is not accompanied by other enhanced decays, however, and since the nature of the 0^+ at 1871 keV is uncertain, the origin of the collectivity in the 2^+ 2766-keV level is unknown, but, given the issues concerning the low-spin three-phonon states, is unlikely to be four-phonon in origin. Possible candidates for non-yrast intruder excitations are the 2^+ level at 2156 keV, with a $B(E2; 2^+ \rightarrow 2_I^+)$ value of 22^{+6}_{-19} W.u. This level, however, also has an enhanced $B(M1)$ for its decay into the 2_1^+ level leading to its identification as a fragment of the 2_{ms}^+ state [28]. The 3^+ level at 2403 keV also has enhanced decays into the 2^+ and 4^+ members of the intruder band, with the $B(E2; 3^+ \rightarrow 2_I^+)$ value being the largest, whereas the calculations predict that the 3^+ intruder level retains its $O(6)$ character to a large degree and thus the corresponding transition should be very weak.

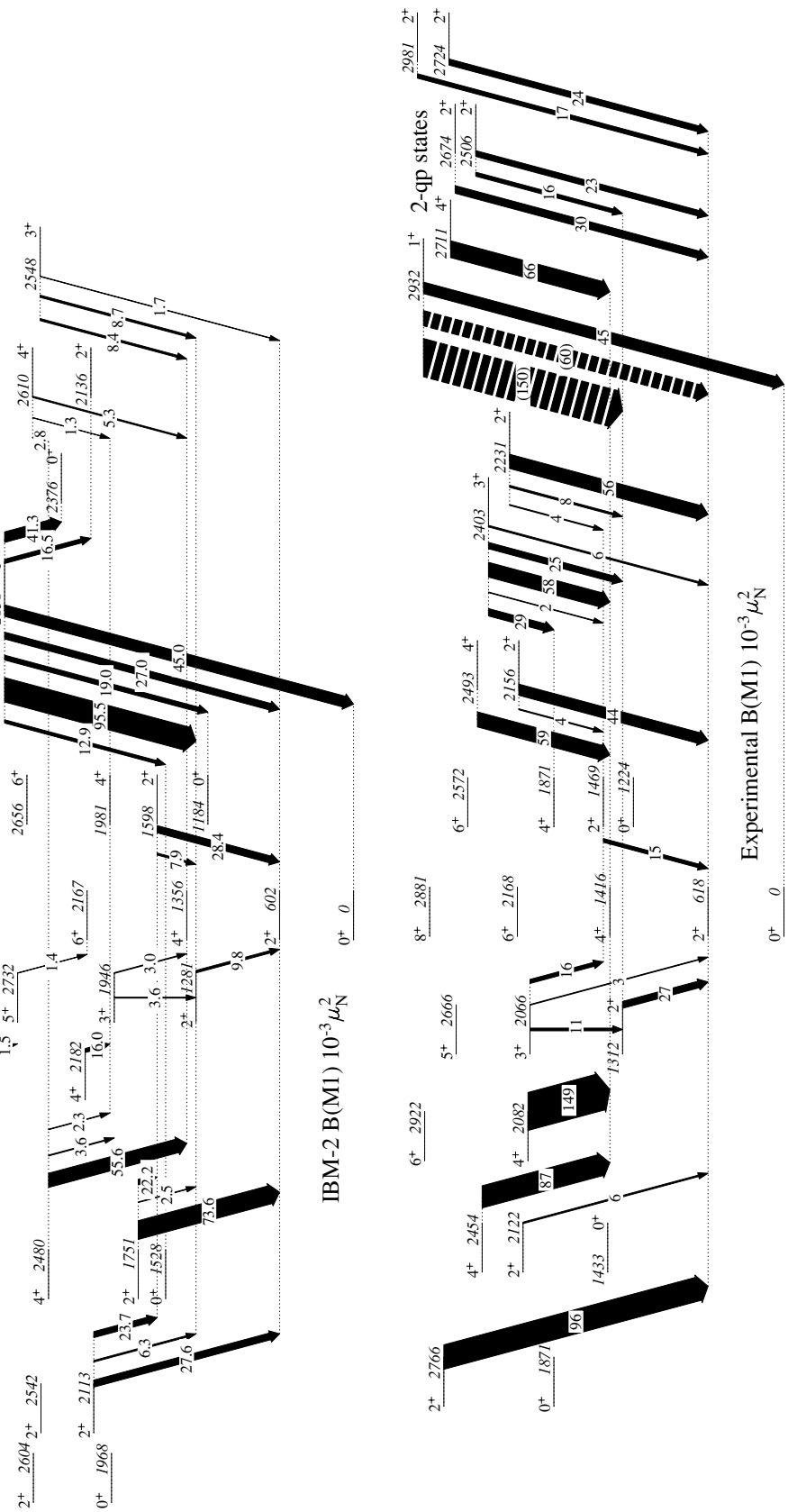

FIG. 16. Results of IBM-2 calculations (top) for selected levels and transitions. The experimental levels (bottom) include those with collective $E2$ transitions as shown in Fig. 14 and also those assigned as two-quasiparticle in nature. Only transitions with $B(M1)$ values greater than 0.001 μ_N^2 are shown and are labeled in units of $10^{-3}\mu_N^2$. Dashed lines indicate upper limits on the $B(M1)$ values.

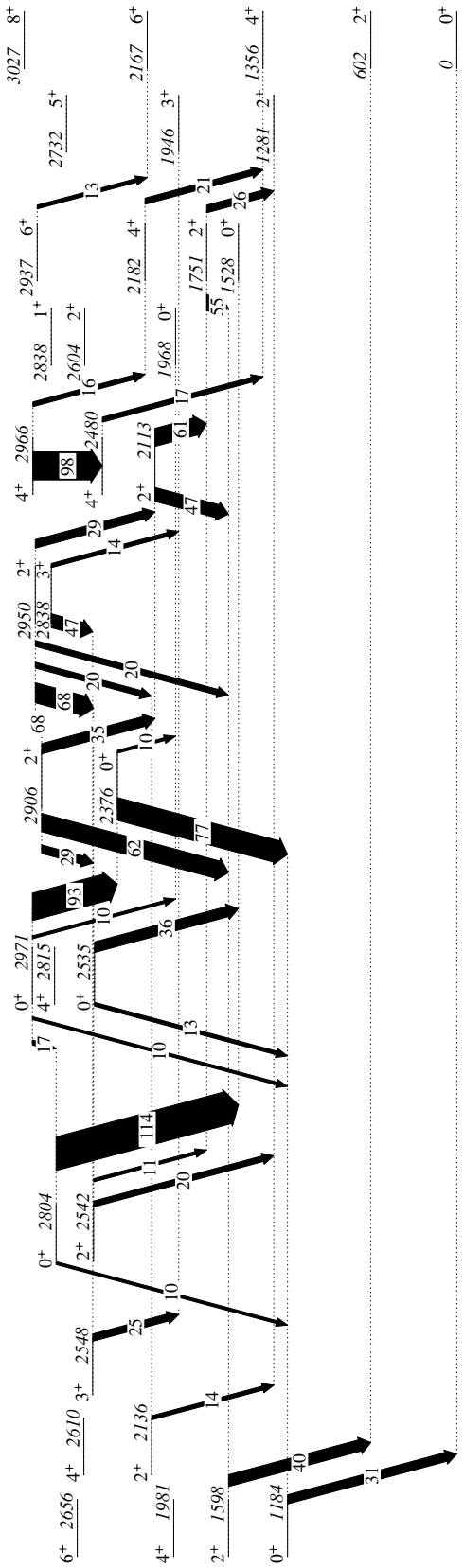

FIG. 17. Results of IBM-2 calculations (described in the text) for states in ^{112}Cd. The transitions are labeled by their $10^{-3}\rho^2(E0)$ values. Only transitions with $\rho^2(E0)$ values greater than 10^{-2} are shown.

Figure 15 displays the results of the calculations for the $B(M1)$ values for levels up to 3 MeV and for transition strengths above 0.01 μ_N^2. The parameters used are those of Délèze *et al.* [42], but the values for the g-factors have been slightly adjusted, keeping the same ratio of g_π/g_ν, in order to reproduce the experimental $B(M1;1^+ \rightarrow 0^+_{\text{g.s.}})$ value of 0.045 μ_N^2. The main fragments of the lowest mixed-symmetry state, experimentally identified as the 2^+_5 and 2^+_6 states at 2156 keV and 2231 keV, are calculated to be located in the $2^+_3, 2^+_4$, and 2^+_5 levels. The calculated strength in the 2^+_3 intruder state arises because of the proximity of the 2^+ three-phonon level and 2^+ mixed-symmetry state. The calculated $\sum_{k=3}^{6} B(M1;2^+_k \rightarrow 2^+_1)$ value of 0.130 μ_N^2 is in very good agreement with the corresponding experimental sum of $0.144^{+0.019}_{-0.017}$ μ_N^2. The calculated $2^+_{ms} \otimes 2^+_{1ph}$ quintuplet, the main source of $M1$ strength, can be observed in Fig. 15 to be located in a series of states in the vicinity of 2.8 MeV. The 1^+ member, calculated at 2838 keV, is experimentally observed at 2932 keV. Unfortunately, the only firm $B(M1)$ value is for the ground-state transition since the other transitions involve mixing ratios that could not be determined — thus only upper limits can be given.

An examination of the experimental data shown in Fig. 16 reveals a number of enhanced $M1$ transitions between low-lying levels that cannot be accounted for in the IBM-2 calculations. In addition, a number of levels that are populated strongly in single-nucleon transfer reactions and identified as two-quasiparticle states also possess significant $M1$ strengths, and are clearly outside the IBM-2 model space. Much of this strength may arise from the $d_{3/2} \rightarrow d_{5/2}$ spin-flip transition involving the two-quasiparticle states and the $d_{5/2}$ component in the 2^+_1 one-phonon wave function. Since experimentally, mixed-symmetry states can only be identified by their enhanced $M1$ decays, which in the Cd nuclei are expected to be rather weak since the $M1$ transition rates are proportional to $N_\pi N_\nu/N^2$ and the N_π and N_ν boson numbers are 1 and 7, respectively, this "background" of quasiparticle contributions makes the assignment of mixed-symmetry states difficult, especially for the $2^+_{1ph} \otimes 2^+_{ms}$ quintuplet. These quasiparticle contributions, however, should not overly influence the transition strength of the $1^+_{ms} \rightarrow 0^+_{\text{g.s.}}$ transition, since the dominant microscopic components involved would necessitate an l-forbidden transition of the form $(s_{1/2} \otimes d_{3/2})^{(1)} \rightarrow (s^2_{1/2})^{(0)}$. Thus, the use of the $1^+_{ms} \rightarrow 0^+_{\text{g.s.}}$ transition to extract the effective boson g factors should not be unduly influenced by quasiparticle amplitudes. Further, the assigned 2^+_{ms} states [28] should also not be affected by this quasiparticle background since no significant $d_{3/2}$ components have been identified in the levels [38,39].

Figure 17 displays the results of the calculations for the $\rho^2(E0)$ values using the parameters of Délèze *et al.* [42], and the effective monopole charges recommended by Giannatiempo *et al.* [55] that were fitted to the ^{110,112,114}Cd isotopes. As already noted, the experimental $\rho^2(E0)$ values from the low-lying levels are reproduced well by the calculations. Unfortunately, $E0$ strengths for levels at higher excitation energy are not available, and thus detailed comparisons cannot be made.

VI. CONCLUSIONS

Levels in ^{112}Cd have been investigated with the $(n, n'\gamma)$ reaction, and level lifetimes have been determined using the Doppler shift attenuation technique. Transition rates have been extracted for γ-ray decays, and levels have been interpreted using the vibrational model with intruding proton $2p4h$ states and two-quasiparticle states. Calculations for the levels and transition rates based on the IBM-2 including mixing between phonon and intruder states have been performed. While there is reasonable agreement at the two-phonon level, whether they are two quadrupole phonons or octupole-quadrupole coupled states as investigated in Ref. [29], the lack of agreement for the higher-phonon levels for all but the yrast states implies that ^{112}Cd should not be used as a paradigm for the $U(5)$ symmetry up to high excitation energy. While the intruder picture is able to describe many features, some subtle cancellations needed, i.e., in the decay of the 0_3^+ and 4_3^+ levels, indicate that some physics is missing. Considered in isolation, the deviations from the vibrational expectations might be explained by incorporating degrees of freedom not taken into account in the present study. Clearly, hexadecapole or g-boson effects must be included, as well as two-quasiparticle degrees of freedom. When taken together with results of detailed Coulomb excitation studies on the Pd isotopes [57,58], it may be suggested that there are no "clean" examples of robust vibrational behavior in the $Z = 46$ or $Z = 48$ nuclei, although the low-lying levels give the appearance of vibrational degrees of freedom. Detailed systematic studies of the Cd isotopes that may shed light on their true natures are in progress.

Future experimental work must concentrate on the extraction of the low-energy decay branches from levels at high-excitation energy to search for additional collective transitions. This could be achieved through detailed β-decay studies of ^{112}Ag and ^{112}In that are planned for the TRIUMF-ISAC facility. Further, a sensitive Coulomb excitation experiment is clearly called for to both verify the reduced transition rates determined in the present study, and also to extract transition matrix elements that could not be determined. In addition, a detailed Coulomb excitation measurement could yield the shape invariants [58] that would allow for an unprecedented view of a collective "vibrational" nucleus.

ACKNOWLEDGMENTS

Support for this work was provided by the U.S. National Science Foundation under grant PHY-0354656, the Swiss National Fund for Scientific Research, the Deutsche forschungsgemeinschaft under grant JO 391/3-2, and the Natural Sciences and Engineering Research Council of Canada.

[1] A. Bohr, Mat. Fys. Medd. K. Dan. Vidensk. Selsk. **26**, 1 (1952).
[2] G. Scharff-Goldhaber and J. Weneser, Phys. Rev. **98**, 212 (1955).
[3] L. Wilets and M. Jean, Phys. Rev. **102**, 788 (1956).
[4] A. Arima and F. Iachello, Phys. Rev. Lett. **35**, 1069 (1975).
[5] A. Arima and F. Iachello, Ann. Phys. (NY) **99**, 253 (1976).
[6] K. Heyde, P. Van Isacker, M. Waroquier, G. Wenes, and M. Sambataro, Phys. Rev. C **25**, 3160 (1982).
[7] P. D. Duval and B. R. Barrett, Nucl. Phys. **A376**, 213 (1982).
[8] J. L. Wood, K. Heyde, W. Nazarewicz, P. Van Duppen, and M. Huyse, Phys. Rep. **215**, 101 (1992).
[9] F. Iachello, in *Proceedings of the 8th International Symposium on Capture Gamma-Ray Spectroscopy and Related Topics*, Fribourg, 1993, edited by J. Kern (World Scientific, Singapore, 1994), p. 3.
[10] J. Jolie and K. Heyde, Phys. Rev. C **42**, 2034 (1990).
[11] K. Heyde, C. De Coster, J. Jolie, and J. L. Wood, Phys. Rev. C **46**, 541 (1992).
[12] K. Heyde, J. Jolie, H. Lehmann, C. De Coster, and J. L. Wood, Nucl. Phys. **A586**, 1 (1995).
[13] J. Jolie and H. Lehmann, Phys. Lett. **B342**, 1 (1995).
[14] H. Lehmann and J. Jolie, Nucl. Phys. **A588**, 623 (1995).
[15] C. De Coster, K. Heyde, B. Decroix, P. Van Isacker, J. Jolie, H. Lehmann, and J. L. Wood, Nucl. Phys. **A600**, 251 (1996).
[16] C. De Coster, B. Decroix, and K. Heyde, Phys. Lett. **B379**, 20 (1996).
[17] H. Lehmann, J. Jolie, C. De Coster, B. Decroix, K. Heyde, and J. L. Wood, Nucl. Phys. **A621**, 767 (1997).
[18] B. Decroix, J. De Beule, C. De Coster, K. Heyde, A. M. Oros, and P. Van Isacker, Phys. Rev. C **57**, 2329 (1998).
[19] B. Decroix, C. De Coster, K. Heyde, A. M. Oros, and J. De Beule, Phys. Rev. C **58**, 232 (1998).
[20] J. Kern, P. E. Garrett, J. Jolie, and H. Lehmann, Nucl. Phys. **A593**, 21 (1995).
[21] F. Corminboeuf, T. B. Brown, L. Genilloud, C. D. Hannant, J. Jolie, J. Kern, N. Warr, and S. W. Yates, Phys. Rev. Lett. **84**, 4060 (2000).
[22] F. Corminboeuf, T. B. Brown, L. Genilloud, C. D. Hannant, J. Jolie, J. Kern, N. Warr, and S. W. Yates, Phys. Rev. C **63**, 014305 (2001).
[23] H. Lehmann, P. E. Garrett, J. Jolie, C. A. McGrath, M. Yeh, and S. W. Yates, Phys. Lett. **B387**, 259 (1996).
[24] L. K. Kostov, W. Andrejtscheff, L. G. Kostova, L. Käubler, H. Prade, and R. Schwengner, Eur. Phys. J. A **2**, 269 (1998).
[25] Yu.N. Lobach, A. D. Efimov, and A. A. Pasternak, Eur. Phys. J. A **6**, 131 (1999).
[26] S. Harissopulos, A. Dewald, A. Gelberg, K. O. Zell, P. von Brentano, and J. Kern, Nucl. Phys. **A683**, 157 (2001).
[27] P. E. Garrett, H. Lehmann, J. Jolie, C. A. McGrath, M. Yeh, W. Younes, and S. W. Yates, Phys. Rev. C **64**, 024316 (2001).
[28] P. E. Garrett, H. Lehmann, C. A. McGrath, M. Yeh, and S. W. Yates, Phys. Rev. C **54**, 2259 (1996).
[29] P. E. Garrett, H. Lehmann, J. Jolie, C. A. McGrath, M. Yeh, and S. W. Yates, Phys. Rev. C **59**, 2455 (1999).
[30] T. Belgya, G. Molnár, and S. W. Yates, Nucl. Phys. **A607**, 43 (1996).
[31] K. B. Winterbon, Nucl. Phys. **A246**, 293 (1975).
[32] W. T. Milner, F. K. McGowan, P. H. Stelson, R. L. Robinson, and R. O. Sayer, Nucl. Phys. **A129**, 687 (1969).
[33] F. K. McGowan, R. L. Robinson, P. H. Stelson, and J. L. C. Ford, Jr., Nucl. Phys. **66**, 97 (1965).
[34] N.-G. Jonsson, J. Kantele, and A. Bäcklin, Nucl. Instrum. Methods **152**, 485 (1978).

[35] D. De Frenne and E. Jacobs, Nucl. Data Sheets **79**, 639 (1996).
[36] H. Lehmann, A. Nord, A. E. de Almeida Pinto, O. Beck, J. Besserer, P. von Brentano, S. Drissi, T. Eckert, R.-D. Herzberg, D. Jäger, J. Jolie, U. Kneissl, J. Margraf, H. Maser, N. Pietralla, and H. H. Pitz, Phys. Rev. C **60**, 024308 (1999).
[37] C. Kohstall, D. Belic, P. von Brentano, C. Fransen, A. Gade, R.-D. Herzberg, J. Jolie, U. Kneissl, A. Linnemann, A. Nord, N. Pietralla, H. H. Pitz, M. Scheck, F. Stedile, V. Werner, and S. W. Yates, Phys. Rev. C **72**, 034302 (2005).
[38] N. Blasi, S. Micheletti, M. Pignanelli, R. de Leo, R. Hertenberger, F. J. Eckle, H. Kader, P. Schiemenz, and G. Graw, Nucl. Phys. **A551**, 251 (1990).
[39] P. D. Barnes, J. R. Comfort, and C. K. Bockelman, Phys. Rev. **155**, 1319 (1967).
[40] L. H. Goldman, J. Kremenek, and S. Hinds, Phys. Rev. **179**, 1172 (1969).
[41] J. Kumpulainen, R. Julin, J. Kantele, A. Passoja, W. H. Trzaska, E. Verho, J. Väärämäki, D. Cutoiu, and M. Ivascu, Phys. Rev. C **45**, 640 (1992).
[42] M. Délèze, S. Drissi, J. Kern, P. A. Tercier, J.-P. Vorlet, J. Rikovska, T. Otsuka, S. Judge, and A. Williams, Nucl. Phys. **A551**, 269 (1993).
[43] M. Délèze, S. Drissi, J. Jolie, J. Kern, and J.-P. Vorlet, Nucl. Phys. **A554**, 1 (1993).
[44] S. Drissi, P. A. Tercier, H. G. Börner, M. Délèze, F. Hoyler, S. Judge, J. Kern, S. J. Mannanal, G. Mouze, K. Schreckenbach, J.-P. Vorlet, N. Warr, A. Williams, and C. Ythier, Nucl. Phys. **A614**, 137 (1997).
[45] R. de Leo, N. Blasi, S. Micheletti, M. Pignanelli, W. T. A. Borghols, J. M. Schippers, S. Y. van der Werf, G. Maino, and M. N. Harakeh, Nucl. Phys. **A504**, 109 (1989).
[46] M. Pignanelli, N. Blasi, S. Micheletti, R. de Leo, M. A. Hofstee, J. M. Schippers, S. Y. van der Werf, and M. N. Harakeh, Nucl. Phys. **A519**, 567 (1990).
[47] M. Pignanelli, N. Blasi, S. Micheletti, R. de Leo, L. LaGamba, R. Perrino, J. A. Bordewijk, M. A. Hofstee, J. M. Schippers, S. Y. van der Werf, J. Wesseling, and M. N. Harakeh, Nucl. Phys. **A540**, 27 (1992).
[48] R. Hertenberger, G. Eckle, F. J. Eckle, G. Graw, D. Hofer, H. Kader, P. Schiemenz, Gh. Cata-Danil, C. Hategan, N. Fujiwara, K. Hosono, M. Kondo, M. Matsuoka, T. Noro, T. Saito, S. Kato, S. Matsuki, N. Blasi, S. Micheletti, and R. de Leo, Nucl. Phys. **A574**, 414 (1994).
[49] H. W. Fielding, R. E. Anderson, C. D. Zafiratos, D. A. Lind, F. E. Cecil, H. H. Weiman, and W. P. Alford, Nucl. Phys. **A281**, 389 (1977).
[50] J. L. Wood, E. F. Zganjar, C. De Coster, and K. Heyde, Nucl. Phys. **A651**, 323 (1999).
[51] R. D. Smith, V. R. Brown, and V. A. Madsen, Phys. Rev. C **33**, 847 (1986).
[52] T. Otsuka, computer programs NPBOS and NPEM (1977).
[53] T. Otsuka, A. Arima, F. Iachello, and I. Talmi, Phys. Lett. **B76**, 139 (1978).
[54] T. Otsuka, A. Arima, and F. Iachello, Nucl. Phys. **A309**, 1 (1979).
[55] A. Giannatiempo, A. Nannini, A. Perego, and P. Sona, Phys. Rev. C **44**, 1844 (1991).
[56] M. Kadi, N. Warr, P. E. Garrett, J. Jolie, and S. W. Yates, Phys. Rev. C **68**, 031306(R) (2003).
[57] L. E. Svensson, C. Fahlander, L. Hasselgren, A. Bäcklin, L. Westerberg, D. Cline, T. Czosnyka, C. Y. Wu, R. M. Diamond, and H. Kluge, Nucl. Phys. **A584**, 547 (1995).
[58] D. Cline, Annu. Rev. Nucl. Part. Sci. **36**, 683 (1986).